

Constraining Majorana CP Phase in Precision Era of Cosmology and Double Beta Decay Experiment

Hisakazu Minakata,^{1,2,*} Hiroshi Nunokawa,^{1,†} and Alexander A. Quiroga^{1,‡}

¹ *Departamento de Física, Pontifícia Universidade Católica do Rio de Janeiro, C. P. 38071, 22452-970, Rio de Janeiro, Brazil*

² *Instituto de Física, Universidade de São Paulo, C. P. 66.318, 05315-970 São Paulo, Brazil*

We show that precision measurement of (1) sum of neutrino masses by cosmological observation and (2) lifetime of neutrinoless double beta decay in ton-scale experiments, with supplementary use of (3) effective mass measured in single beta decay experiment, would allow us to obtain information on the Majorana phase of neutrinos. To quantify the sensitivity to the phase we use, in addition to the conventional allowed region plots, the CP exclusion fraction, a fraction of the CP phase parameter space that can be excluded for a given set of assumed input parameters, a global measure for CP violation. We illustrate the sensitivity under varying assumptions, from modest to optimistic ones, on experimental errors and theoretical uncertainty of nuclear matrix elements. We find that in the latter case one of the two Majorana phases (denoted as α_{21}) can be constrained rather strongly by excluding $\simeq 10 - 50\%$ of the phase space at 3σ CL for the lowest neutrino mass of 0.1 eV. The characteristic features of the sensitivity to α_{21} , such as dependences on the other phase α_{31} and on the true values of α_{21} , are addressed. We also raise the question of whether the uncertainties of nuclear matrix elements could be constrained by consistency of such measurement.

PACS numbers: 14.60.Lm, 14.60.Pq, 13.15.+g, 98.80.Es

I. INTRODUCTION

After all the angles in the lepton mixing matrix [1] and the mass squared differences of neutrinos are determined by the atmospheric, the solar, the reactor, as well as the accelerator neutrino oscillation experiments, we have entered into a new phase of neutrino physics [2–4]. Of course, we are still with the important unknowns in the lepton sector, CP violating phase of Kobayashi-Maskawa type [5] and the neutrino mass hierarchy. Yet, we do have relatively clearer view of how these questions are to be settled, either through the ongoing searches, or by new measurement to be carried out by the powerful apparatus described in various experimental proposals to date.

It is quite possible that even after these unknown quantities are measured by experiments there will still remain the questions of somewhat different category: What are the absolute masses of neutrinos? Are neutrinos Dirac or Majorana particles? If Majorana, which values of the Majorana CP phases [6–8] are chosen by nature? The first one, knowing the absolute mass scale, is crucial to understand physics behind the origin of neutrino mass, and the latter two are likely the key to understand baryon number asymmetry in the universe [9].

In this paper, we focus on detectability of the Majorana CP phase in the light of informations to be obtained by cosmological observation and neutrino experiments in the coming precision era. In particular, in the near future the double beta decay experiments aim to cover entire region of parameters allowed by the inverted mass hierarchy. (See Fig. 1.) We show that given the future perspective, when combined with precision measurement in cosmology, one can indeed expect the sensitivity, though limited one, to one of the phases (denoted as α_{21} , see section II A). We hope that this result can trigger renewed interests in the problem of detectability of the Majorana phase despite the dominant pessimism which prevailed in the past decades. See, however, e.g., Refs. [10–21] for the foregoing efforts which examined the sensitivity to the Majorana phase.

We feel that now is the particularly right time to revisit these issues because of the following reasons. Firstly, cosmological observations entered into the precision era so that their data became sensitive to the absolute masses of neutrinos better than the current bounds from laboratory experiments, as seen most notably by the results obtained by the Planck collaboration [22]. See also Ref. [23] for overview and many relevant references. It makes us possible to employ a new strategy that the neutrino mass scale can be constrained mainly by cosmology and we can use data of neutrinoless double beta decay experiments, with supplementary use of single beta decay data, to constrain the Majorana phases of neutrinos. Even more interestingly a discrepancy between the cosmic microwave background

*Electronic address: hisakazu.minakata@gmail.com

†Electronic address: nunokawa@puc-rio.br

‡Electronic address: alarquis@fis.puc-rio.br

(CMB) and lensing observations about cluster correlations would prefer massive neutrinos with mass of a few tenth of eV [24]. If confirmed, it would make the basis of our analysis more robust.

Secondly, as mentioned above, several new neutrinoless double beta decay experiments are in line to measure or constrain, the ee element of neutrino mass matrix in the flavor basis, so called the effective Majorana mass, to a few tens of meV [25–32]. For reviews and description of the other projects, see e.g., Refs. [33–35]. Needless to say, they are the prime candidates among various experiments that can measure or constrain the Majorana phases. We should also note that intensive efforts have been devoted in order to improve the calculations of the nuclear matrix element (NME) which is crucial to determine the value of effective Majorana mass from the measured half life time in double beta decay experiments [36–39]. See, also Ref. [35] for review of the recent progress in the calculations of NME.

Thirdly, the uncertainties in the relevant lepton mixing angles get decreased dramatically recently. The error of $\sin^2 \theta_{12}$ is now only $\sim 4\%$ [40], and moreover it will be decreased to a sub-% level by future medium-baseline reactor experiments [41, 42]. θ_{13} , the mixing angle whose value was unknown until intriguing indication from T2K [43] by seeing ν_e appearance events, is now precisely measured [44, 45], and it will soon reach to a even greater precision, the error of $\sin^2 \theta_{13}$ would become $\sim 5\%$ level. See Fig. 1 to know how small is the effect of the current uncertainties of the mixing parameters onto the allowed regions by double and single beta decay experiments. These developments are important to tighten up the constraint on Majorana CP phases and to place it on a firmer ground.

In addition, the single beta decay experiment KATRIN [46] (see also [47]) will constrain neutrino masses to a level of 0.2 eV at 90 % CL, or observe the effects consistent with masses of this order, in a manner quite complementary to cosmological observations. While enjoying the above new inputs, our analysis is nothing but a continuation of the numerous similar analyses attempted by the many authors, from which we are certainly benefited.

To display the sensitivities to the Majorana CP phases in a more global way, we use in this paper the CP exclusion fraction f_{CPX} , which is defined as a fraction of the CP phase space that can be excluded for a given set of input parameters [48]¹. In addition to f_{CPX} plots, we also use the more conventional one, the allowed regions of phases for given input parameters and experimental setup which demonstrate how well the input parameters can be reproduced. The CP exclusion fraction is a useful tool particularly in the initial era of search for effects of the Majorana CP phase, in which even the partial exclusion of allowed range of the phase would be very valuable. On the other hand, f_{CPX} has intimate connection to the error of CP phase, an appropriate measure in precision measurement era, as discussed in [48]. It suggests that the CP exclusion fraction can be a universally usable measure for CP sensitivity.

In the following two sections, II and III, we briefly review the basic features of the observables used and describe simple analytic estimation of the effects of Majorana phases. The expert readers must go directly to the results in sections VI and VII, starting from describing the analysis method in section IV.

II. ASSUMPTIONS AND OBSERVABLES USED IN THE ANALYSIS

In this work we assume that the neutrinos are of Majorana type, and the Majorana mass is the unique source of neutrinoless double beta decay. We also assume the standard three-flavor mixing scheme of neutrinos.

In our analysis we consider three observables [51]: (1) the effective neutrino mass (denoted as $m_{0\nu\beta\beta}$) measured by neutrinoless double beta decay experiments, (2) the sum of the neutrino masses (denoted as Σ) which can be determined by cosmological observations, and (3) the effective neutrino mass (denoted as m_β) measured by single beta decay experiments. They are all sensitive to the absolute neutrino mass scale. The sensitivity to the Majorana CP violating phase, which is of our main concern in this paper, primarily comes from $m_{0\nu\beta\beta}$ in (1). But we will see that the other two, in particular Σ in (2), greatly help enhancing the sensitivity. Let us briefly describe their current status.

A. Effective mass for neutrinoless double beta decay

The rate of neutrinoless double beta decay (hereafter denoted as $0\nu\beta\beta$ decay), or the inverse of the half life time of the $0\nu\beta\beta$ decay, $T_{1/2}^{0\nu}$, can be written as

$$[T_{1/2}^{0\nu}]^{-1} = G_{0\nu} \left| \mathcal{M}^{(0\nu)} \right|^2 \left(\frac{m_{0\nu\beta\beta}}{m_e} \right)^2, \quad (1)$$

¹ In Ref. [48] it was used to display sensitivity to the lepton Kobayashi-Maskawa phase achievable in the ongoing long-baseline neutrino oscillation experiments. For earlier discussion of a CP sensitivity measure closely related to f_{CPX} see Refs. [49, 50].

where $G_{0\nu}$ is the kinematic phase space factor, $\mathcal{M}^{(0\nu)}$ is the nuclear matrix element (NME) corresponding to the $0\nu\beta\beta$ transition and m_e is the electron mass. The effective neutrino mass $m_{0\nu\beta\beta}$ measured by $0\nu\beta\beta$ decay experiments is given by

$$m_{0\nu\beta\beta} = \left| m_1 |U_{e1}|^2 + m_2 |U_{e2}|^2 e^{i\alpha_{21}} + m_3 |U_{e3}|^2 e^{i\alpha_{31}} \right| = \left| m_1 c_{13}^2 c_{12}^2 + m_2 c_{13}^2 s_{12}^2 e^{i\alpha_{21}} + m_3 s_{13}^2 e^{i\alpha_{31}} \right|, \quad (2)$$

where m_i ($i = 1, 2, 3$) are neutrino masses and U_{ek} ($k = 1, 2, 3$) are the element of electron-row of the Maki-Nakagawa-Sakata (MNS) neutrino mixing matrix [1], α_{21} and α_{31} are the Majorana CP phases and $c_{ij} \equiv \cos \theta_{ij}$, $s_{ij} \equiv \sin \theta_{ij}$. Throughout this work, as we did in the second equality in Eq. (2), we use the standard parameterization of the MNS matrix including the Majorana phases [52]². We note that while $G_{0\nu}$ can be calculated very accurately as performed, e.g., in Refs. [53, 54], $\mathcal{M}^{(0\nu)}$ is not known very well, the fact which should be taken into account as we will see below.

So far there is no convincing evidence for $0\nu\beta\beta$ decay or non-zero value of $m_{0\nu\beta\beta}$. Though it was claimed by the authors of Ref. [55] that they saw a positive signal at more than 4σ CL which is consistent with $m_{0\nu\beta\beta} = 0.2 - 0.6$ eV, it does not appear to become a consensus in the community. The result is not confirmed by GERDA [27] which used the same nuclei ^{76}Ge . Furthermore, a combined analysis of EXO [25] and KamLAND-Zen [26] data, both using ^{136}Xe , results in the upper limit of the effective mass

$$m_{0\nu\beta\beta} < 0.1 - 0.25 \text{ eV} \quad (90\% \text{ CL}) \quad (3)$$

which appears to exclude the above claim at a confidence level higher than 97.5% [26]. Fortunately, the sensitivity to $m_{0\nu\beta\beta}$ in the ongoing and the next generation $0\nu\beta\beta$ decay experiments will go down to the region of a few tens of meV [33]. These experiments would eventually cover an entire region expected for the inverted mass hierarchy (see Fig. 1), and the controversy will certainly be settled on the way toward the goal.

The largest uncertainty in translating the bounds on $T_{1/2}^{0\nu}$ to that of $m_{0\nu\beta\beta}$ comes from the uncertainty of the NME, $\mathcal{M}^{(0\nu)}$, which produces typically a factor of ~ 2 or more differences in terms of $m_{0\nu\beta\beta}$. Despite that a lot of efforts have been devoted, there are still some considerable differences among NME values obtained by different authors and by different calculation methods. Generally speaking, the difference between different authors is not very large if the same calculation technique is used. The best hope would be to normalize the coupling strength by using the 2ν decay by which the difference may go down to $\simeq 30\%$ level, as proposed within the framework of quasi-particle random phase approximation (QRPA) method [36, 37]. But, notable difference persists to among results calculated by different techniques³.

B. Sum of neutrino masses

For our purpose, in addition to $m_{0\nu\beta\beta}$, it is crucial to take into account the sum of the neutrino masses, Σ ,

$$\Sigma \equiv m_1 + m_2 + m_3, \quad (4)$$

which can be determined by cosmological observations. So far, in most of the analyses of the cosmological data, there has not been any clear evidence of non-zero value of Σ and only its upper bounds were obtained. Here, as our reference, we only refer the bounds recently obtained by Planck collaboration at 95% CL [22]:

$$\Sigma < \begin{cases} 0.98 \text{ eV} & (\text{Planck} + \text{WMAP} + \text{CMB}), \\ 0.32 \text{ eV} & (\text{Planck} + \text{WMAP} + \text{CMB} + \text{BAO}), \end{cases} \quad (5)$$

where the first limit was obtained by combining the Planck data with that coming from WMAP, CMB polarization data, and the second limit was obtained by adding also the data of baryon acoustic oscillation (BAO) (see Ref. [22] for details). In deriving these bounds, deviation from the flat universe was allowed.

² Strictly speaking, using the standard parameterization of the MNS matrix found in [52], the CP phase appears in the term proportional to m_3 in Eq. (2) is $\alpha_{31} - 2\delta$ where δ is the Kobayashi-Maskawa type CP phase but for simplicity, we redefine this quantity as α_{31} .

³ It appears that the QRPA method [39, 56, 57] and the interacting boson model [58, 59] systematically lead to larger NME values than that calculated by the interacting shell model [60, 61]. See e.g., Table I and Fig. 1 of Ref. [62] in which a comparison between the NME values obtained by these models is made.

However, more recently, some analyses are in favour of non-zero Σ which could be attributed to the sub-eV masses of the active or sterile neutrinos [24, 63, 64]. In Ref. [24] it was discussed that a discrepancy between CMB and lensing observations about cluster correlations prefers massive neutrinos leading to the preferred non-zero value as $\Sigma = 0.32 \pm 0.081$ eV, which implies that $m_1 \sim m_2 \sim m_3 \sim 0.1$ eV in the standard three flavour scheme. We expect that some future cosmological data either from galaxy surveys or weak lensing data by the Euclid satellite, with Planck constraints, may lead to the sensitivity to $\Sigma \simeq 0.01\text{--}0.05$ eV [65–68].

Despite the success in tightening up the neutrino mass bound by cosmological data we should keep in mind that the analysis has done (or needs to be done) with certain prior or within a cosmological model such as the standard Λ CDM model.

C. Effective mass for beta decay

In addition to the observables mentioned above, the absolute neutrino mass scale can also be probed by the single beta decay experiment, which measures the effective electron neutrino mass, m_β , defined as

$$m_\beta \equiv [m_1^2 |U_{e1}|^2 + m_2^2 |U_{e2}|^2 + m_3^2 |U_{e3}|^2]^{\frac{1}{2}} = [m_1^2 c_{13}^2 c_{12}^2 + m_2^2 c_{13}^2 s_{12}^2 + m_3^2 s_{13}^2]^{\frac{1}{2}}, \quad (6)$$

providing us information independent of cosmology and $0\nu\beta\beta$ decay experiment. So far there is no evidence of non-zero value of m_β and only the upper bounds,

$$m_\beta < \begin{cases} 2.3 \text{ eV} & (95\%\text{CL; Mainz collaboration}) \\ 2.05 \text{ eV} & (95\%\text{CL; Troitsk collaboration}) \end{cases}, \quad (7)$$

have been obtained by Mainz [69] and Troitsk [70] collaborations. In the near future, we expect that this bound can be improved by one order of magnitude by KATRIN [46] which is expected to reach the sensitivity of $m_\beta \sim 0.2$ eV at 90% CL.

D. Allowed regions of $m_{0\nu\beta\beta}$ and m_β as a function of lightest neutrino mass

In this paper we use the lightest neutrino mass (rather than Σ), denoted as m_0 , as the relevant parameter (observable) to be determined by the experiments. Namely, $m_0 \equiv m_1$ and $m_0 \equiv m_3$ for the normal and the inverted mass hierarchies, respectively. All the other masses and their differences can be calculated by using the relations

$$m_1 \equiv m_0, \quad m_2 = \sqrt{m_0^2 + \Delta m_{21}^2}, \quad m_3 = \sqrt{m_0^2 + \Delta m_{21}^2 + \Delta m_{32}^2} \quad (\text{normal mass hierarchy}), \quad (8)$$

$$m_1 = \sqrt{m_0^2 - \Delta m_{21}^2 - \Delta m_{32}^2}, \quad m_2 = \sqrt{m_0^2 - \Delta m_{32}^2}, \quad m_3 \equiv m_0 \quad (\text{inverted mass hierarchy}), \quad (9)$$

where $\Delta^2 m_{ij} \equiv m_i^2 - m_j^2$ ($i, j = 1, 2, 3$). Notice that Δm_{32}^2 in Eq. (9) for the case of inverted mass hierarchy is a *negative* quantity.

While our results are insensitive to small variation of the mixing parameters we use, for definiteness, the values obtained in [71] will be used as our reference parameters throughout this work:

$$\begin{aligned} \Delta m_{21}^2 &= 7.54 \times 10^{-5} \text{ eV}^2, \\ \sin^2 \theta_{12} &= 0.308 \text{ or } \sin^2 2\theta_{12} = 0.853, \end{aligned} \quad (10)$$

for both mass hierarchies whereas

$$\begin{aligned} \Delta m_{32}^2 &= 2.40 \text{ } (-2.44) \times 10^{-3} \text{ eV}^2, \\ \sin^2 \theta_{13} &= 0.0234 \text{ } (0.0239) \text{ or } \sin^2 2\theta_{13} = 0.0914 \text{ } (0.0933), \end{aligned} \quad (11)$$

for the normal (inverted) mass hierarchy⁴. For later convenience we define $\Delta m_{\text{atm}}^2 \equiv |\Delta m_{32}^2|$. Using these values of the parameters $m_{0\nu\beta\beta}$ at its current status can be summarized as

$$m_{0\nu\beta\beta} \simeq |0.676 \text{ } (0.675) m_1 + 0.301 m_2 e^{i\alpha_{21}} + 0.0234 \text{ } (0.0239) m_3 e^{i\alpha_{31}}| \quad (12)$$

⁴ Since the best fitted values of mass squared difference for atmospheric neutrino oscillation, Δm^2 , shown in Table I of Ref. [71], is defined as $\Delta m^2 \equiv m_3^2 - (m_1^2 + m_2^2)/2$, the values of Δm_{32}^2 in Eq. (11) were obtained by using the relation $\Delta m_{32}^2 = \Delta m^2 - \Delta m_{21}^2/2$.

for the normal (inverted) mass hierarchy.

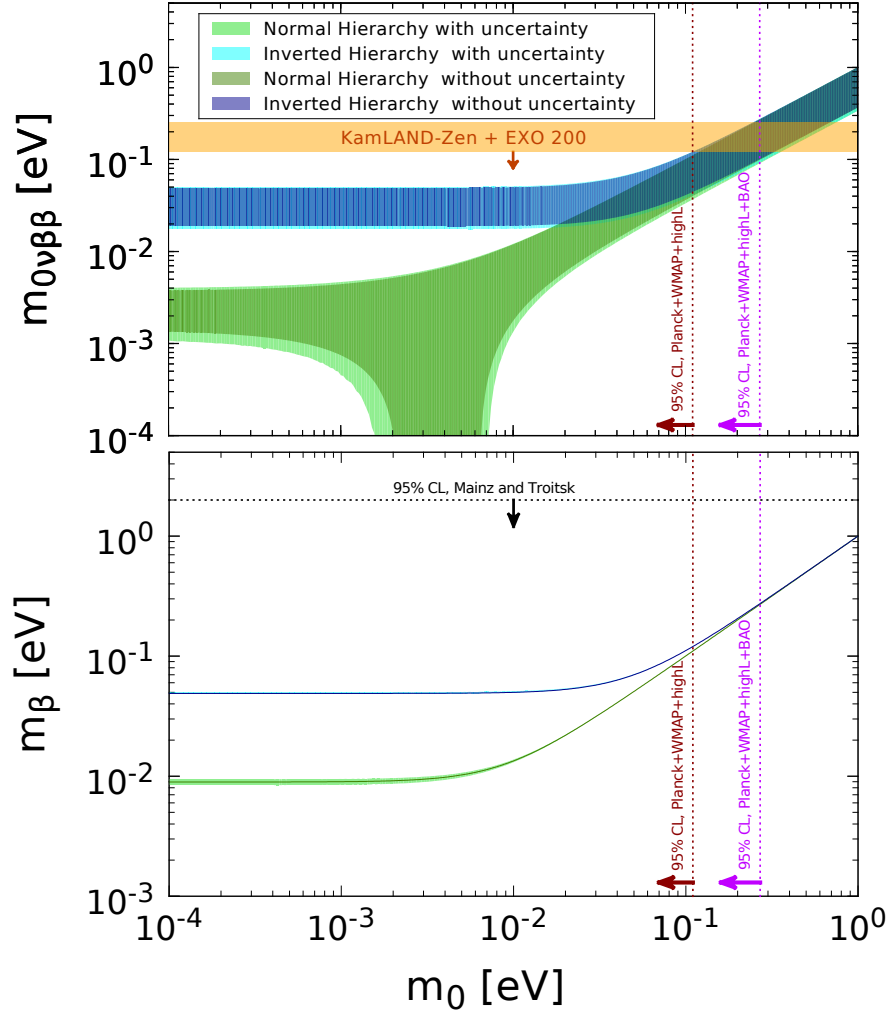


FIG. 1: The currently allowed ranges of $m_{0\nu\beta\beta}$ (upper panel) and m_β (lower panel), observables of $0\nu\beta\beta$ decay and single beta decay experiments, respectively, are shown as a function of the lightest neutrino mass m_0 . In the case of normal (inverted) mass hierarchy the ranges are shown by green (blue) colour. In the both panels, the light (dark) coloured regions are computed by taking into account (without taking account) the current 1σ uncertainties of the relevant mixing parameters. Also shown are the limits on $m_{0\nu\beta\beta}$ coming from KamLAND-Zen and EXO [26] (by the light brown band and arrow), the bounds on m_0 obtained by Planck collaboration [22] (by the magenta and the brown dotted lines), and also the upper limit on m_β coming from Mainz [69] and Troitsk [70] experiments (by the black dotted line).

In Fig. 1, we show the allowed ranges of $m_{0\nu\beta\beta}$ and m_β as a function of m_0 for both the normal and the inverted mass hierarchies. The allowed ranges are calculated by the two ways, without and with the current 1σ uncertainties of the mixing parameters, which are indicated, respectively, by the dark and light colours, blue and green for the inverted and normal hierarchy. Notice that the effect of 1σ uncertainties of the mixing parameters is quite small by now. In contrast, additional variation over the Majorana phases α_{21} and α_{31} gives much larger impact on $m_{0\nu\beta\beta}$, not only producing sizeable width but also creating a down-going branch in region $10^{-3} \text{ eV} \lesssim m_0 \lesssim 10^{-2} \text{ eV}$ for the case of the normal mass hierarchy due to the strong cancellation of the three mass terms in Eq. (2).

The difference between the normal and the inverted mass hierarchies becomes clearly visible only in small m_0 region, typically $m_0 \lesssim 0.1 \text{ eV}$ in the both plots. Therefore, onset to the almost degenerate mass regime, which is formally defined as $m_0 \gg \sqrt{\Delta m_{\text{atm}}^2} \simeq 0.05 \text{ eV}$, already takes place for $m_{0\nu\beta\beta}$ and m_β at around $m_0 \gtrsim 0.1 \text{ eV}$.

In the same plots, we also show the limits on $m_{0\nu\beta\beta}$ coming from KamLAND-Zen and EXO [26] (by the light brown band and arrow), the bounds on m_0 obtained by Planck collaboration [22] (shown by the magenta and the brown dotted lines), and also the upper limit on m_β coming from Mainz [69] and Troitsk [70] experiments (shown by the black dotted line). We note that the upper limit on $m_{0\nu\beta\beta}$ provided by KamLAND and EXO is expressed by the

band (not by line) because of the NME uncertainty.

III. ANALYTIC ESTIMATE OF THE EFFECT OF MAJORANA PHASE

In this section, we discuss qualitative features of effects of the Majorana phase onto the $0\nu\beta\beta$ decay observable $m_{0\nu\beta\beta}$. It is partly for pedagogical purpose but we hope that some new points presented serve for better understanding the results to be obtained in later sections. In particular, we aim at illuminating how and where the best sensitivity to the Majorana phase can be expected. After briefly mentioning a general properties of $m_{0\nu\beta\beta}$ we will focus on this problem.

A. Reduction of Majorana phase space

We give here a general properties of $m_{0\nu\beta\beta}$ in Eq. (2). Since the phases α_{21} and α_{31} enter into $m_{0\nu\beta\beta}$ in the form of either one of $\cos\alpha_{21}$, $\cos\alpha_{31}$, and $\cos(\alpha_{31} - \alpha_{21})$ $m_{0\nu\beta\beta}$ has the following reflection symmetry

$$m_{0\nu\beta\beta}(m_0, \alpha_{21}, \alpha_{32}) = m_{0\nu\beta\beta}(m_0, 2\pi - \alpha_{21}, 2\pi - \alpha_{32}). \quad (13)$$

Notice that it is the simultaneous transformation of two phase variables and each one of α_{21} or α_{31} does not obey individually the symmetry under $\alpha_{ij} \rightarrow 2\pi - \alpha_{ij}$.

B. The case of almost degenerate mass spectra

The best place to discuss clearly how and where the best sensitivity to the Majorana phase can be expected is in the almost degenerate regime, $m_1 \approx m_2 \approx m_3$, as ensured if $m_0 \gg \sqrt{\Delta m_{\text{atm}}^2} \simeq 0.05$ eV, where $\Delta m_{\text{atm}}^2 \equiv |\Delta m_{32}^2|$. Moreover, the regime turns out to be the main target of our analysis, given reasonable values of experimental errors in the next generation $0\nu\beta\beta$ decay experiments. The effective mass $m_{0\nu\beta\beta}$ in Eq. (2) in this regime is given approximately to leading order in s_{13}^2 as

$$m_{0\nu\beta\beta} \simeq c_{13}^2 m_0 \times \left[1 - \sin^2 2\theta_{12} \sin^2 \left(\frac{\alpha_{21}}{2} \right) + \frac{1}{2} \sin^2 2\theta_{13} \{ c_{12}^2 \cos \alpha_{31} + s_{12}^2 \cos(\alpha_{21} - \alpha_{31}) \} \right]^{\frac{1}{2}}. \quad (14)$$

for the both mass hierarchies. The dominant effect of the Majorana phase is induced by α_{21} because the last term in the square bracket in Eq. (14) is smaller than the first terms by a factor of 10 – 20. Ignoring the $\sin^2 2\theta_{13}$ term, the maximum and minimum values of $m_{0\nu\beta\beta}$ (upper and lower edges of the bands for $m_0 \gtrsim 0.1$ eV in the plot in Fig. 1) are simply given, respectively, by

$$m_{0\nu\beta\beta}^{\text{max}} \simeq c_{13}^2 m_0, \quad m_{0\nu\beta\beta}^{\text{min}} \simeq c_{13}^2 m_0 \cos 2\theta_{12} \simeq 0.383 m_{0\nu\beta\beta}^{\text{max}}. \quad (15)$$

It means that the ratio of the maximum to the minimum value of effective mass changes by a factor of $m_{0\nu\beta\beta}^{\text{max}}/m_{0\nu\beta\beta}^{\text{min}} \simeq 2.6$ as the Majorana phase is varied. Therefore, if one can determine $m_{0\nu\beta\beta}$ from experiment with errors smaller than the factor 2.6, after taking into account the uncertainty coming from the NME, it is in principle possible to constrain the Majorana phase α_{21} .

Then, the question is: In what regions of α_{31} the best sensitivity to α_{21} can be expected? We are primarily interested in the sensitivity to α_{21} because the sensitivity to α_{31} itself is quite low in our setting, due to the small value of θ_{13} , as we will see in later sections. As the sensitivity to the phase arises in places where the NME uncertainty cannot obscure the effect of phases the best place is at the maximal and the minimal value of $m_{0\nu\beta\beta}$. One can show that $m_{0\nu\beta\beta}$ in Eq. (14) is nearly periodic function of α_{21} and α_{31} , and has the following properties in regions $0 \leq \alpha \leq \pi$: (1) The function inside parenthesis in Eq. (14) is an extremely slowly decreasing function of α_{31} for in the entire region of α_{21} . (2) It is a decreasing function of α_{21} in the entire region of α_{31} , and varies from $\simeq 1$ to $\simeq 0.15$ as α_{31} is varied from 0 to π . Therefore, it has the maximum (minimum) at $\alpha_{21} = \alpha_{31} = 0$ ($\alpha_{21} = \alpha_{31} = \pi$). Thus, the best sensitivity to α_{21} is obtained at either $\alpha_{31} = 0$ or π . On the contrary, the worst sensitivity is expected at around the mean value of $m_{0\nu\beta\beta}$ between their maximum and minimum values. Typically, they are at around $\alpha_{21} \simeq 2\pi/3$ for the whole range of α_{31} . These features will be confirmed explicitly by quantitative analysis in later sections.

C. Hierarchical case; inverted mass spectrum

Now let us consider the case of $m_0 < \sqrt{\Delta m_{21}^2} \lesssim 0.01$ eV for the inverted mass ordering. In this case, $m_1 \approx m_2 \sim \sqrt{\Delta m_{\text{atm}}^2} \gg m_3 \equiv m_0$. This is the regime corresponding to the horizontal band for the inverted mass spectra in Fig. 1. It is interesting to observe that essentially the same treatment can go through for $m_{0\nu\beta\beta}$ in these two entirely different mass spectra. In the case of strongly hierarchical inverted mass spectrum the m_3 term in Eq. (12) is suppressed than other two terms by a factor of $m_3/m_2 \ll [\Delta m_{21}^2/\Delta m_{\text{atm}}^2]^{1/2} \simeq 0.18$ and $s_{13}^2 = 0.0234$ (0.0239) for the normal (inverted) hierarchy. In the case of almost degenerate spectrum the suppression of m_3 term is only due to the latter factor.

Under the approximation of ignoring the m_3 term, $m_{0\nu\beta\beta}$ is expressed as in the degenerate case, (14) without s_{13}^2 term, but replacing m_0 by $\sqrt{\Delta m_{\text{atm}}^2}$,

$$m_{0\nu\beta\beta} \simeq c_{13}^2 \sqrt{\Delta m_{\text{atm}}^2} \left[1 - \sin^2 2\theta_{12} \sin^2 \left(\frac{\alpha_{21}}{2} \right) \right]^{\frac{1}{2}}. \quad (16)$$

Since the dependence of $m_{0\nu\beta\beta}$ on the Majorana phase is essentially the same as in the case of the degenerate mass regime, the same results hold for the sensitivity to α_{21} and the location of highest sensitivity. Under our assumption of the precision of $\delta(m_{0\nu\beta\beta}) \equiv \sigma_{0\nu\beta\beta} = 0.01$ eV (see section IV), however, the sensitivity to α_{21} is quite limited in this regime when it is combined with the NME uncertainty. It will be demonstrated in the analysis in section VII.

D. Hierarchical case; normal mass spectrum

If $m_0 \ll \sqrt{\Delta m_{21}^2}$, typically $m_0 \sim 10^{-4}$ eV, one can ignore $m_1 (= m_0)$ term in Eq. (12). Then, we obtain the expression of $m_{0\nu\beta\beta}$ as

$$m_{0\nu\beta\beta} = \sqrt{\Delta m_{21}^2} \left[s_{12}^4 c_{13}^4 + 2\sqrt{\frac{s_{13}^4}{\epsilon}} s_{12}^2 c_{13}^2 \cos(\alpha_{31} - \alpha_{21}) \right]^{1/2} \simeq \sqrt{\Delta m_{21}^2} [0.905 + 0.0801 \cos(\alpha_{31} - \alpha_{21})]^{1/2} \quad (17)$$

where $\epsilon \equiv \Delta m_{21}^2/\Delta m_{\text{atm}}^2 \simeq 0.0314$ and we have kept order $\sqrt{s_{13}^4/\epsilon}$ term which is $\simeq 0.13$, but ignored the terms of order ϵ^2 , $s_{13}^4/\epsilon \simeq 5.3 \times 10^{-4}/0.0314 \simeq 0.017$ and $\sqrt{\epsilon} s_{13}^2 \simeq 4.1 \times 10^{-3}$. Thus, in the normal mass hierarchy with small m_0 region, the phase α_{31} (in a combination $\alpha_{31} - \alpha_{21}$) affects the $0\nu\beta\beta$ decay rate, in contrast to the case of almost degenerate and inverted hierarchy mass spectra in which only α_{21} plays a role. As α_{31} changes $m_{0\nu\beta\beta}$ varies as

$$\sqrt{\Delta m_{21}^2} \left[s_{12}^4 c_{13}^4 - 2\sqrt{\frac{s_{13}^4}{\epsilon}} s_{12}^2 c_{13}^2 \right]^{1/2} \leq m_{0\nu\beta\beta} \leq \sqrt{\Delta m_{21}^2} \left[s_{12}^4 c_{13}^4 + 2\sqrt{\frac{s_{13}^4}{\epsilon}} s_{12}^2 c_{13}^2 \right]^{1/2} \quad (18)$$

Or numerically,

$$0.105\sqrt{\Delta m_{21}^2} \simeq 9.11 \times 10^{-4} \text{ eV} \leq m_{0\nu\beta\beta} \leq 0.412\sqrt{\Delta m_{21}^2} \simeq 3.58 \times 10^{-3} \text{ eV} \quad (19)$$

a factor of ~ 4 variation. Again, under our assumption of the precision of $\sigma_{0\nu\beta\beta} = 0.01$ eV it would be very difficult to probe the value of α_{31} in this regime, as we will see in section VII.

IV. ANALYSIS METHOD

Throughout this paper, unless otherwise stated, we use the mixing parameters described in Eqs. (10) and (11). We do not consider the uncertainties of the mixing parameters apart from the currently unknown mass hierarchy, because the impact is rather small which is expected to become even smaller in the near future. This is because we expect significant improvement in the accuracies of these parameters by future oscillation experiments, in particular, by the medium baseline ($\sim 50 - 60$ km) reactor experiments such as JUNO [41] and RENO-50 [42] as demonstrated, e.g., in Refs. [72–75].

A. Assumption on experimental errors

As discussed in the previous sections, we use the three observables, sum of neutrino masses Σ , and the effective mass parameters m_β and $m_{0\nu\beta\beta}$ which are measured, respectively, in single and double beta decay experiments. Let us assume that they are measured with some uncertainties around the central values, $\Sigma^{(0)}$, $m_\beta^{(0)}$ and $m_{0\nu\beta\beta}^{(0)}$:

$$\Sigma^{\text{obs}} = \Sigma^{(0)} \pm \sigma_\Sigma, \quad (20)$$

$$m_\beta^{\text{obs}} = m_\beta^{(0)} \pm \sigma_\beta, \quad (21)$$

$$m_{0\nu\beta\beta}^{\text{obs}} = m_{0\nu\beta\beta}^{(0)} \pm \sigma_{0\nu\beta\beta}, \quad (22)$$

where σ_Σ , σ_β and $\sigma_{0\nu\beta\beta}$ denote the corresponding 1σ uncertainties. We take the following values for the uncertainties,

$$\sigma_\Sigma = 0.05 \text{ eV}, \quad \sigma_\beta = 0.06 \text{ eV}, \quad \sigma_{0\nu\beta\beta} = 0.01 \text{ eV}, \quad (23)$$

which will be used as the reference values in our analysis.

Here is some reasonings for our choices of the uncertainties in Eq. (23). It appears that future galaxy surveys [65] and weak lensing [66] both lead, under the Planck constraint, the sensitivity to Σ to the level of $0.03 - 0.05$ eV. According to Ref. [68], in the most optimistic case, the sensitivity could even lead to ~ 0.01 eV. Therefore, our choice would be in a conservative side. For KATRIN [47] they quote the error 0.025 eV^2 for m_β^2 , which may be translated into the error of 0.063 eV for m_β for the case where true value of $m_0 = 0.2 \text{ eV}$, which justifies our choice in Eq. (23).

To have a reasonable estimate of the uncertainty in $m_{0\nu\beta\beta}$ we need a detailed discussion because we must address the question of how the experimental uncertainty on $T_{1/2}^{0\nu}$ is translated into that of $m_{0\nu\beta\beta}$, and the treatment heavily depend on to what extent the experimental backgrounds can be suppressed. We present such a discussion in Appendix A, based, e.g. on Refs.[35, 76]. Under the assumption of dominance of statistical error, we will argue there that the uncertainty of 0.01 eV may be reachable in future experiments that are upgraded to a ton scale. Such experiments will be able to cover the entire allowed range corresponding to the inverted mass hierarchy.

B. Analysis procedure

As we emphasized in section II A the error of $m_{0\nu\beta\beta}$ due to uncertainties of the NME would be a major obstacle to extract informations of the Majorana phases from $0\nu\beta\beta$ decay experiments. Therefore, its treatment is of key importance in our analysis to constrain the Majorana phases. We follow the procedure similar to the one used in Ref. [19].

Let us assume that the unknown true value of NME, denoted as $\mathcal{M}^{(0\nu)}$, is restricted to some range as

$$\mathcal{M}_{\min}^{(0\nu)} \leq \mathcal{M}^{(0\nu)} \leq \mathcal{M}_{\max}^{(0\nu)}, \quad (24)$$

where $\mathcal{M}_{\min}^{(0\nu)}$ and $\mathcal{M}_{\max}^{(0\nu)}$ denote the minimum and maximum possible values of NME, respectively. Then, we introduce the NME uncertainty parameter $r_{\text{NME}} \equiv \mathcal{M}_{\max}^{(0\nu)} / \mathcal{M}_{\min}^{(0\nu)}$. If we arbitrarily define the reference value $\mathcal{M}_0^{(0\nu)}$ as the geometric mean,

$$\mathcal{M}_0^{(0\nu)} \equiv \left(\mathcal{M}_{\max}^{(0\nu)} \mathcal{M}_{\min}^{(0\nu)} \right)^{1/2}, \quad (25)$$

$\mathcal{M}_{\max}^{(0\nu)}$ and $\mathcal{M}_{\min}^{(0\nu)}$ can be written as

$$\mathcal{M}_{\max}^{(0\nu)} = \sqrt{r_{\text{NME}}} \mathcal{M}_0^{(0\nu)}, \quad \mathcal{M}_{\min}^{(0\nu)} = \frac{1}{\sqrt{r_{\text{NME}}}} \mathcal{M}_0^{(0\nu)}. \quad (26)$$

Notice that $r_{\text{NME}} = 1$ implies no uncertainty on NME.

We take into account of the uncertainties of NME via the following way. Using Σ , m_β , and $m_{0\nu\beta\beta}$ in Eqs. (20) - (22), we define the χ^2 function as follows,

$$\chi^2 \equiv \min \left\{ \left[\frac{\Sigma^{(0)} - \Sigma^{\text{fit}}}{\sigma_\Sigma} \right]^2 + \left[\frac{m_\beta^{(0)} - m_\beta^{\text{fit}}}{\sigma_\beta} \right]^2 + \left[\frac{\xi m_{0\nu\beta\beta}^{(0)} - m_{0\nu\beta\beta}^{\text{fit}}}{\sigma_{0\nu\beta\beta}} \right]^2 \right\}, \quad (27)$$

where

$$\xi \equiv \frac{\mathcal{M}_0^{(0\nu)}}{\mathcal{M}^{(0\nu)}}, \quad (28)$$

will be varied in the interval of $[1/\sqrt{r_{\text{NME}}}, \sqrt{r_{\text{NME}}}]$, and the minimization will be done with respect to m_0 , α_{21} , α_{31} and ξ . In this way, the NME uncertainty is treated in a similar way as the systematic error. (It is very similar to the treatment of a normalization parameter to take into account of the flux uncertainty in reactor neutrino experiments.) In this work, we consider three values of the NME uncertainty parameter, $r_{\text{NME}} = 1.3, 1.5$ and 2.0 . (Exceptional use of an extreme value, $r_{\text{NME}} = 1.1$, is made at the end of section VII.) We note that, strictly speaking, errors associated to the three observables we consider in this work are not Gaussian, in particular, the one comes from cosmology. It would be proper to do analysis based on Monte Carlo simulations, as performed, e.g., in Refs. [80, 81]. However, we believe that the procedure we use produces approximately correct results, which are sufficient for our purpose.

Currently, for a given nuclei, the typical ratio of the maximum to minimum NME calculated by different techniques are about the factor of 2. So we consider $r_{\text{NME}} = 2.0$ as the current situation. We assume that in the future, theoretical uncertainty on the NME could be reduced to 50% or even to 30%, which may be possible if the main source/reason of the discrepancies of the NME values calculated by different techniques are identified. We expect that once the positive signal of $0\nu\beta\beta$ will be observed by using different isotopes, by comparing the real data from these different isotopes, it would be possible to check in a systematic way the validity of various theoretical calculations based on different models or methods, which may allow to reduce significantly the NME uncertainty.

Using the χ^2 function defined in Eq. (28), we will determine the allowed parameter space by imposing the condition,

$$\Delta\chi^2 \equiv \chi^2 - \chi_{\text{min}}^2 < 2.3, 6.18 \text{ and } 11.83 \text{ (1, 4 and 9)} \quad (29)$$

for 1, 2 and 3 σ CL for two (one) degree of freedom.

C. Plotting allowed regions and CP exclusion fraction

In the following two sections we will present our analysis results. In section VI we display the allowed regions for some combinations of the assumed true (input) values of m_0 , α_{21} and α_{31} . In section VII we present the contours of equal CP exclusion fraction f_{CPX} . It is defined [48] as the fraction of values of $\alpha_{21} \in [0, 2\pi]$ which can be excluded by the experiments at a given confidence level for each input point of the parameter space (m_0, α_{21}) . The f_{CPX} contour plot can be defined for phase α_{31} as well. It is thus a global measure which covers the entire input parameter space. For more precise definition of f_{CPX} see Ref. [48].

V. HOW CAN THE MAJORANA PHASES BE CONSTRAINED?

One may ask why and how the Majorana phases can be constrained in the presence of NME uncertainty ξ in Eq. (27). Before presenting our main results let us make a short discussion and present some results of our analysis on this point because it illuminates how the NME uncertainty can be circumvented at least partly.

For clarity we focus on the case of almost degenerate mass spectrum discussed in section III B. In this case $m_{0\nu\beta\beta}$ prepared by nature is related to the “observed” one, the inferred one with use of particular NME (using Eq. (14) without the terms which contains $\sin^2 2\theta_{13}$) as

$$m_{0\nu\beta\beta}^{\text{obs}} = \xi^{-1} m_{0\nu\beta\beta}^{\text{true}} \simeq \xi^{-1} c_{13}^2 m_0 \left[1 - \sin^2 2\theta_{12} \sin^2 \left(\frac{\alpha_{21}}{2} \right) \right]^{\frac{1}{2}}. \quad (30)$$

Since ξ enters into Eq. (30) in combination with m_0 , if we are completely ignorant about m_0 , there is no way to constrain the value of α_{21} even in the case of no NME uncertainty ($\xi = 1$) no matter how accurately $m_{0\nu\beta\beta}$ itself is determined. Therefore, in order to measure the Majorana phases, it is of crucial importance to determine m_0 from

the other observation different from $0\nu\beta\beta$ decay⁵. We will show below that the major role is played by cosmological observation.

Assuming that m_0 is determined with good accuracy, change of $m_{0\nu\beta\beta}^{\text{true}}$ in Eq. (30) as α_{21} is varied is of a factor of $\simeq 2.6$ (see section III B). The phase information can be gained only if the NME uncertainty ξ cannot compensate the variation. Thus, we expect that sensitivity to the Majorana phase is maximal at the true value of α_{21} at 0 or π where $m_{0\nu\beta\beta}^{\text{true}}$ has extremal values in the case of degenerate mass spectrum.

Let us examine relative contribution of each experiment in constraining the Majorana phase, α_{21} . In Fig. 2 we show the values of $\Delta\chi^2$ as a function of fitted values of α_{21} for the case of inverted (left panel) and normal (right panel) mass hierarchies. The true values of parameters are taken as $m_0 = 0.1$ eV, $\alpha_{21} = \pi$ and $\alpha_{31} = 0$, and the errors of measurement are taken as assumed in Eq. (23) for all the three experiments. The dotted blue and the dashed green lines indicate, respectively, $\Delta\chi^2$ obtained if we only consider $0\nu\beta\beta$ decay experiment only and $0\nu\beta\beta + \beta$ decay experiments.

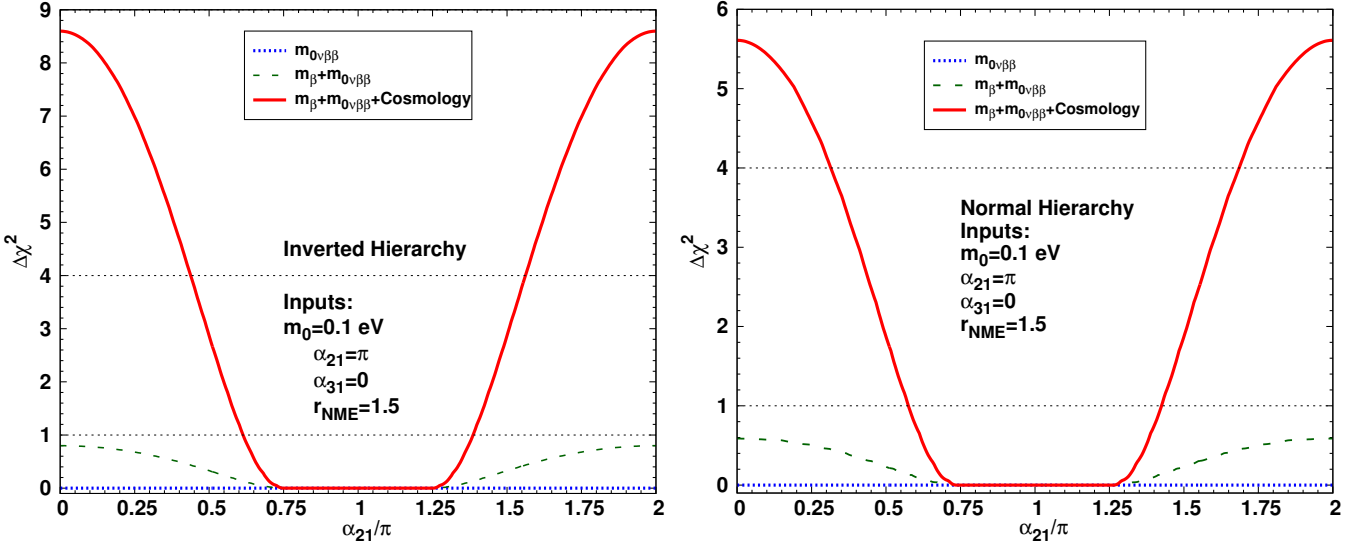


FIG. 2: $\Delta\chi^2$ is plotted as a function of the fitted value of α_{21} for the case of the inverted (left panel) and normal (right panel) mass hierarchies. Notice that the scale of the vertical axis is different between the left and right panels. The true values of the parameters are taken as $m_0 = 0.1$ eV, $\alpha_{21} = \pi$, and $\alpha_{31} = 0$. The three $\Delta\chi^2$ curves are presented which correspond to three combinations of the data used in the analysis, only $0\nu\beta\beta$ decay (dotted blue line), $0\nu\beta\beta + \beta$ decays (dashed green curve) and all combined, $0\nu\beta\beta + \beta$ decays + cosmology (solid red curve). In the fit the remaining parameters, m_0 and α_{31} , are marginalized.

First we confirm that the contribution from the $0\nu\beta\beta$ decay alone can not determine or constrain at all the value of α_{21} (see blue dotted lines in Fig. 2) which is true even if there is no NME uncertainty. Even if the result of beta decay is added to that of $0\nu\beta\beta$, the restricting power of α_{21} is very weak as we can see from the green dashed lines. However, once the cosmological observation of Σ is added $\Delta\chi^2$ jumps outside the region $0.6\pi - 1.4\pi$ of α_{21} as shown by solid red curve in Fig. 2. Therefore, it is the precision measurement of Σ , of course together with $0\nu\beta\beta$ decay experiments, to produce nontrivial constraint on α_{21} by circumventing the NME uncertainty. We note that at the bottom of $\Delta\chi^2$ in region $\alpha_{21} = 0.75\pi - 1.25\pi$, χ_{min}^2 is very flat because of the NME uncertainty. This means that it is impossible to pin down, in the presence of the NME uncertainty, the value of the Majorana phase α_{21} at the bottom no matter how accurately all the measurements are done.

We also observe that the sensitivity to the Majorana phase is higher for the inverted mass hierarchy. This is because, for a given value of m_0 , the first and second terms which contain m_1 and m_2 , respectively, in Eq. (2) are always larger in the case of inverted hierarchy than the ones in the normal one, as we can see from Eqs. (8) and (9). Assuming the difference between $|\Delta m_{32}^2|$ in both mass hierarchies is small, as is the case in Eq. (11), it makes $\Delta\chi^2$ for the inverted mass hierarchy larger, thereby making the inverted hierarchy case more sensitive to the change of α_{21} .

⁵ We note, however, that this is not always true for the non-degenerate case where in some situation, it would be possible to constrain the CP phase only using the information from $0\nu\beta\beta$ decay experiment.

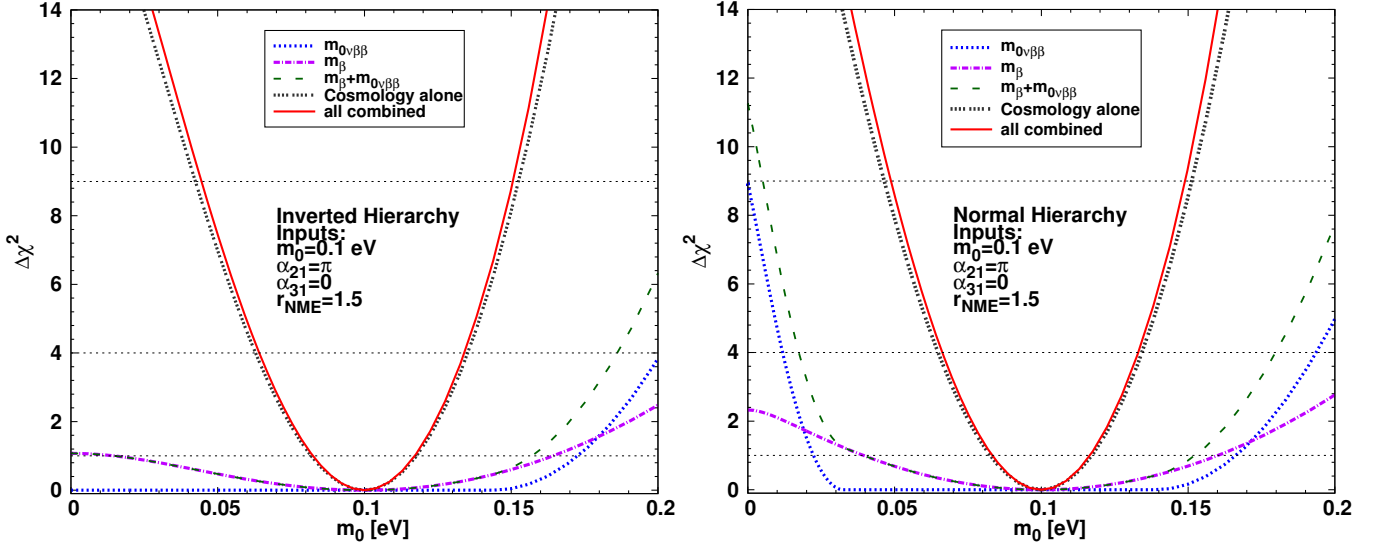


FIG. 3: Similar plots as in Fig. 2 but as a function of the fitted value of m_0 for the five combinations of the data set used in the analysis.

Let us also examine the contribution from each experiment to the determination of m_0 . In Fig. 3 we show $\Delta\chi^2$ obtained by marginalizing the other parameters as a function of the fitted value of m_0 for the case of inverted (left panel) and normal (right panel) mass hierarchies. Here, we present five (out of seven) possible combinations in the plot. Again the contribution from cosmology dominates the $\Delta\chi^2$ curve and the contribution from $0\nu\beta\beta$ decay is visible only in the region $m_0 \gtrsim 0.15$ eV for the inverted mass hierarchy and $m_0 \lesssim 0.03$ eV and $m_0 \gtrsim 0.15$ eV for the normal mass hierarchy.

We conclude that $0\nu\beta\beta$ experiments and cosmological observation work together in a very complementary fashion to produce nontrivial constraints on the Majorana phase. In the case of inverted mass hierarchy with hierarchical spectrum, m_0 in Eq. (30) is to be replaced by $\sqrt{\Delta m_{\text{atm}}^2}$, and the same treatment goes through.

VI. ANALYSIS RESULTS I: ALLOWED REGIONS OF m_0 , α_{21} AND α_{31}

In this section, we study the sensitivity to the CP phase through the conventional plots of allowed regions, which indicate how accurately one can reproduce the assumed input parameters. Let us first consider, for the purpose of illustration, the case where the true values of relevant fundamental parameters are, $m_0 = 0.1$ ($\Sigma \simeq 0.32$ eV) and $\alpha_{21} = \alpha_{31} = \pi$. In Fig. 4 the allowed regions projected into the planes of (a) $\alpha_{21} - m_0$ (b) $\alpha_{21} - \alpha_{31}$ and (c) $m_0 - \alpha_{31}$ are drawn. The NME uncertainty is taken as $r_{\text{NME}} = 1.5$. In the case of inverted mass hierarchy they are depicted by the filled colours, yellow, red, and light blue, corresponding, respectively, to 1, 2 and 3 σ CL for 2 degree of freedom (DOF). While for the normal mass hierarchy they are drawn by the black dotted (1 σ), dashed (2 σ) and the solid (3 σ) curves.

We first notice that for both mass hierarchies, it is possible to restrict α_{21} in some interval at 2 σ CL (for 2 DOF) but no constraint on α_{21} can be placed at 3 σ CL as we can see from the panels (a) and (b) of Fig. 4. On the other hand, as expected, it is not possible to constrain at all the phase α_{31} due to the small value of θ_{13} , see Eq. (12). We have checked that this is true even if we consider different true values of α_{31} , where the dependence of the allowed regions on α_{31} is always very mild. We also note that the allowed regions in Fig. 4(b) are symmetric with respect to $\alpha_{21} = \pi$ in a good approximation. It stems from the simultaneous reflection symmetry $\alpha_{21} \rightarrow 2\pi - \alpha_{21}$ and $\alpha_{31} \rightarrow 2\pi - \alpha_{31}$ in Eq. (13) and the weak dependence of $\Delta\chi^2$ on α_{31} .

In Fig. 5 we show the same plots as in Fig. 4 but for different value of $m_0 = 0.2$ eV ($\Sigma \simeq 0.61$ eV). In this case, as we can see in Fig. 4(a) and (b) that we can constrain α_{21} significantly better than the case of $m_0 = 0.1$ eV for the both mass hierarchies. We note that indeed the difference between the normal and inverted mass hierarchy is very small for $m_0 = 0.2$ eV, which is expected as it is in the almost degenerate regime.

Since the dependence on α_{31} is quite mild, from now on we will show only the allowed regions projected into the plane of $\alpha_{21} - m_0$, which is the most interesting combination for our purpose. In Fig. 6 we show the regions allowed

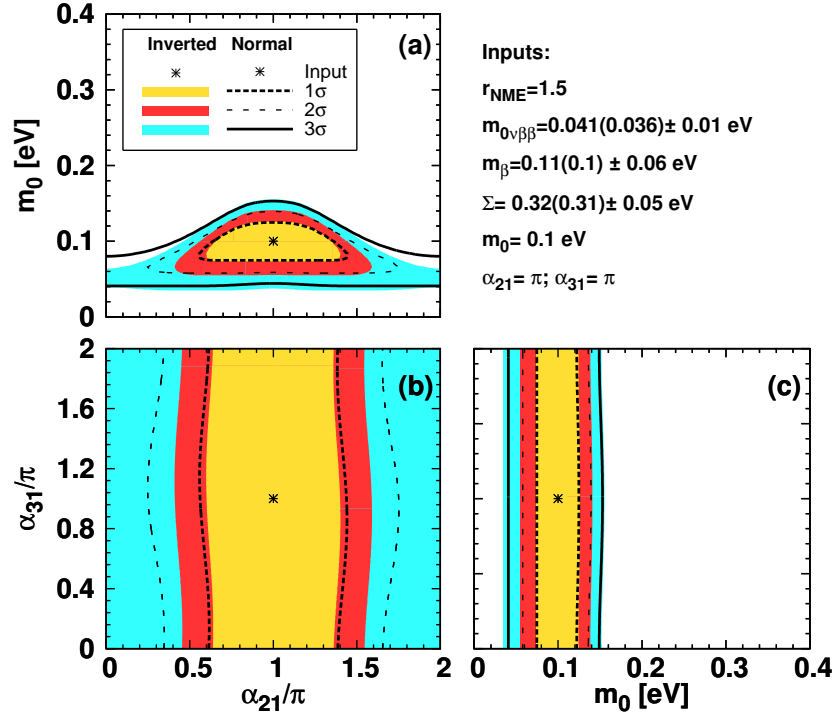


FIG. 4: Regions allowed at 1, 2 and 3 σ CL indicated by the filled color of yellow, red and light blue, respectively, for 2 DOF, projected into the planes of (a) $\alpha_{21} - m_0$ (b) $\alpha_{21} - \alpha_{31}$ and (c) $m_0 - \alpha_{31}$ for the case of the inverted mass hierarchy and the true values of $m_0 = 0.1$ eV, $\alpha_{21} = \alpha_{31} = \pi$, and $r_{\text{NME}} = 1.5$. The allowed contours of the normal mass hierarchy are shown by the dotted (1 σ), dashed (2 σ), and solid (3 σ) curves. In the legend, the numbers outside (inside) the parentheses corresponds to the inverted (normal) mass hierarchy.

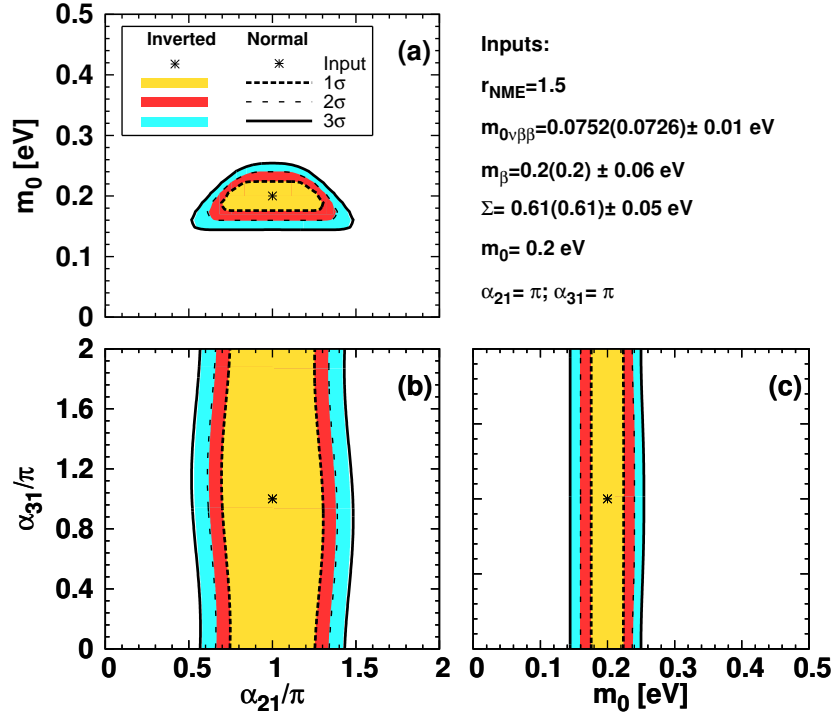


FIG. 5: Same as in Fig. 4 but for the case where $m_0 = 0.2$ eV.

at 2 σ CL for 2 DOF, projected into the plane of $\alpha_{21} - m_0$. The first, second, third and the fourth rows in Fig. 6

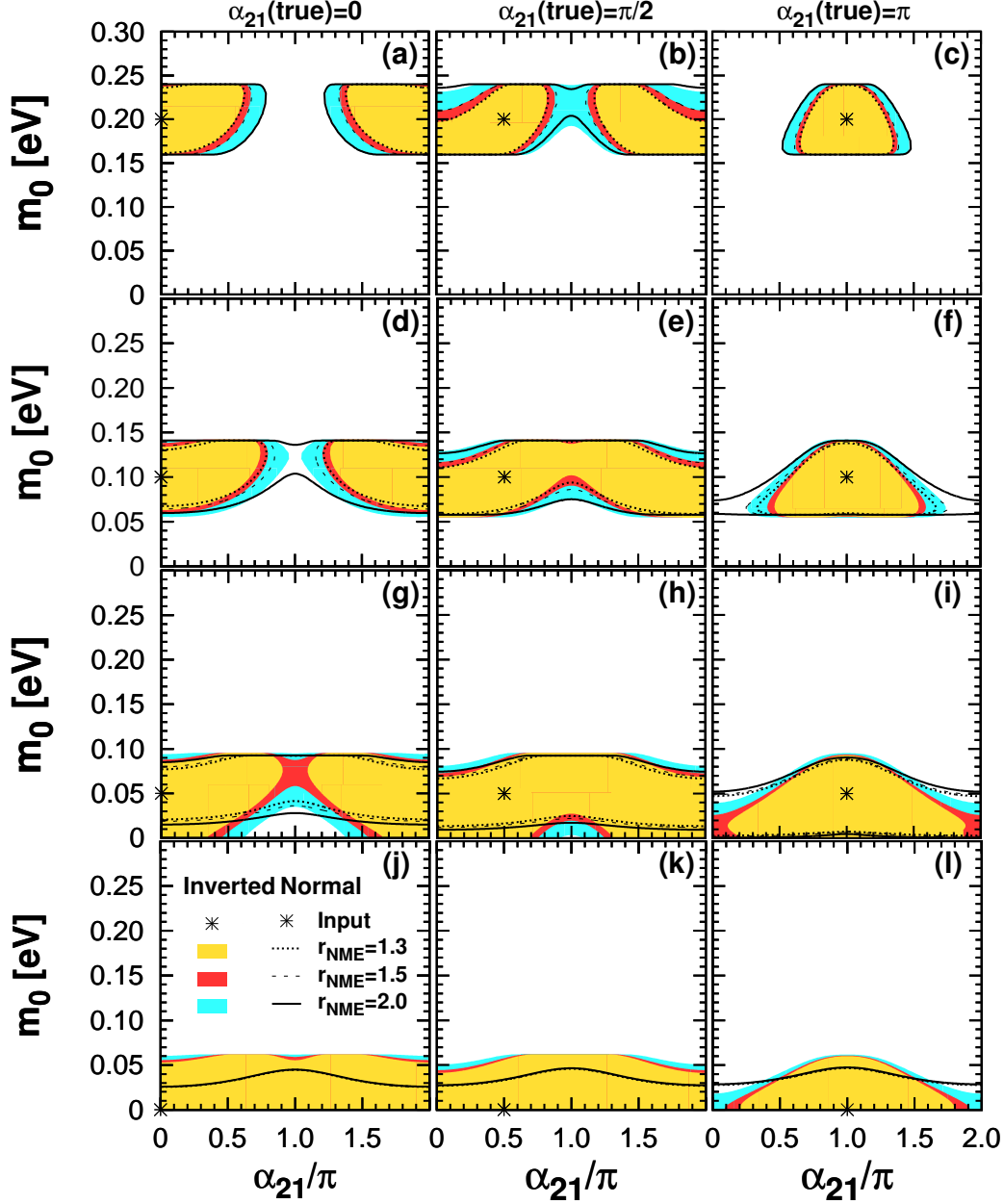


FIG. 6: Regions allowed at 2σ CL for 2 DOF, projected into the plane of $\alpha_{21} - m_0$ for the cases where the true values of $(m_0/\text{eV}, \alpha_{21}) =$ (a) (0.2, 0), (b) (0.2, $\pi/2$), (c) (0.2, π), (d) (0.1, 0), (e) (0.1, $\pi/2$), (f) (0.1, π), (g) (0.05, 0), (h) (0.05, $\pi/2$), (i) (0.05, π), (j) (0.0, 0), (k) (0.0, $\pi/2$) and (l) (0.0, π), indicated by the symbol of asterisk. The true value of α_{31} was set to π for all the cases. The case of the inverted mass hierarchy is indicated by the filled colours, yellow, red, and light blue, corresponding to $r_{\text{NME}} = 1.3, 1.5$, and 2.0 , respectively. Whereas for the case of normal mass hierarchy, the contours are shown by the solid, dotted, and the dashed lines corresponding, respectively, to $r_{\text{NME}} = 1.3, 1.5$ and 2.0 .

correspond to the cases where the true values of $m_0 = 0.2$ eV, 0.1 eV, 0.05 eV, and 0.0 eV, respectively. The left, middle, and right panels in Fig. 6 are for the cases where the true values of $\alpha_{21} = 0$, $\alpha_{21} = \pi/2$, and $\alpha_{21} = \pi$, respectively. The input values are indicated by the asterisks. The allowed regions for the inverted mass hierarchy for $r_{\text{NME}} = 1.3, 1.5$ and 2.0 are indicated by filled colors of yellow, red, and light blue, respectively, whereas that for normal mass hierarchy are indicated by the black dotted, dashed and solid curves, respectively.

We first note that due to the marginalization with respect to α_{31} , the allowed regions in Fig. 6 show the reflection symmetry around $\alpha_{21} = \pi$. Generally speaking the sensitivity to α_{21} is higher for larger m_0 . The exception is the case of the inverted hierarchy with $m_0 = 0$ eV and the input $\alpha_{21} = \pi$, where the allowed contour is slightly smaller than that of the same hierarchy with $m_0 = 0.05$ eV. Among the input values of α_{21} considered for Fig. 6, the sensitivity

to α_{21} is highest (though modest) for $\alpha_{21}(\text{true}) = \pi$ and lowest for $\alpha_{21}(\text{true}) = \pi/2$, which is consistent with our expectation described in section III B. Even in the highest sensitivity case examined (top row) the allowed region cannot be smaller than a third of the range of α_{21} . On the other hand, the sensitivity to α_{21} still persists even for m_0 less than 0.05 eV. We note, however, if the allowed (or excluded) range of α_{21} is evaluated for 1 DOF, which is reasonable if we are interested in restricting only the single parameter α_{21} , as we will do in the next section, the sensitivity would become better.

As we can see in the first and the second rows of Fig. 6, the difference between normal and inverted hierarchies is quite small if the parameter m_0 is well within the degenerate regime, $m_0 = 0.2$ eV, but it starts to develop when m_0 is increased to 0.1 eV, as we can see in the first and second rows of Fig. 6. For m_0 smaller than $\simeq 0.05$ eV, the difference between the hierarchies become more visible, as can be seen in third and fourth rows of Fig. 6.

Let us finally comments also on the determination of m_0 . We first observe that the allowed ranges of m_0 for a given input value of m_0 do not depend essentially on the assumed input values of α_{21} in agreement with our expectation as m_0 is mainly determined by cosmological observation coming from the constraint on Σ . We further note that if $m_0(\text{true}) = 0.05$ eV and the true mass hierarchy is inverted, it is not possible to exclude the case of $m_0 = 0$ at 2σ CL even for $r_{\text{NME}} = 1.3$. This is because if the hierarchy is inverted, the case of $m_0(\text{true}) = 0.05$ eV, or equivalently $\Sigma(\text{true}) = 0.19$ eV, is compatible with $m_0(\text{fit}) = 0$ since in this case the sum of the other 2 masses give $m_1 + m_2 \simeq 0.14$ eV. On the other hand, for the normal hierarchy, $m_3 \simeq 0.05$ eV alone is not sufficient to mimic the case of $m_0(\text{true}) = 0.05$ eV, which is equivalent to $\Sigma(\text{true}) \simeq 0.17$ eV for the cases where $\alpha_{21} = 0$ and $\pi/2$ (see the panels (g) and (h) of Fig. 6).

VII. ANALYSIS RESULTS II: CP EXCLUSION FRACTION

In this section, we show the results on the CP exclusion fraction f_{CPX} , which is defined as a fraction of the CP phase parameter space that can be excluded for a given set of input (true) parameter set of $(m_0, \alpha_{21}, \alpha_{31})$ and the NME uncertainty. As discussed in Ref. [48], this is a global measure of CP violation, which we believe particularly useful in the stage where the sensitivity to the CP phase is not so high.

We show in Fig. 7 the iso-contours of the CP exclusion fraction determined at 2σ (95.45%) CL in the plane spanned by the true values of α_{21} and the lightest neutrino mass m_0 for $r_{\text{NME}} = 2.0, 1.5$, and 1.3 from left to right, and the cases where the true values of α_{31} is 0 and π shown, respectively, in the upper and lower panels⁶. Since the iso-contours of f_{CPX} are symmetric under reflection around $\alpha_{21} = \pi$ after marginalizing over α_{31} due to the symmetry in Eq. (13), from now on, we show the results only for the range of $0 \leq \alpha_{21} \leq \pi$. In Fig. 7 the iso-contours of f_{CPX} for the inverted and the normal mass hierarchies are depicted, respectively, by the solid and the dashed lines, from 0.1 to 0.7 (with the step size of 0.1), using different colors as indicated in the legend. Notice that larger the values of f_{CPX} , higher the sensitivity to α_{21} because larger fraction of the phase space can be excluded. We note that for each point on the input parameter space, all the parameters, $m_0, \alpha_{21}, \alpha_{31}$ and ξ were varied in doing the fit.

In each panels in Fig. 7, the sensitivity is highest in region around $\alpha_{21} \simeq \pi$ and next highest in region of α_{21} near 0. The worst sensitivity is obtained at around $\alpha_{21} \sim 2\pi/3$, in agreement with the qualitative discussion given in section III. As expected the difference between the normal and the inverted mass hierarchies are small in the degenerate regime, $m_0 \gtrsim 0.1$ eV where the solid (inverted mass hierarchy) and dashed lines (normal mass hierarchy) overlap rather well.

It is also notable that the case of $\alpha_{31}(\text{true}) = \pi$ (upper panels of Fig. 7) provides somewhat better sensitivity at around $\alpha_{21} = \pi$ than in the case of $\alpha_{31}(\text{true}) = 0$ (lower panels) whereas this behaviour is contrary for the value around $\alpha_{21} = 0$ for which the results in the lower panels provides somewhat better sensitivity (see also the footnote 6). However, the differences are not so large, or the α_{31} dependence is quite weak, which may be anticipated from Eq. (14) due to small θ_{13} . Since we will not be able to know the true value of α_{31} in our current set up (no restriction on α_{31}), in reality, we must assume that the real value of f_{CPX} is somewhere between the results shown in the upper and lower panels of Fig. 7.

It is interesting to see that the sensitivity to α_{21} strongly depends upon r_{NME} . In particular the improvement of the sensitivity from $r_{\text{NME}} = 2.0$ to $r_{\text{NME}} = 1.5$ is remarkable. At $m_0 = 0.15$ eV, for example, while $f_{\text{CPX}} \geq 0.3$ region spans only $\simeq 0.2$ of α_{21} space for $r_{\text{NME}} = 2.0$, it jumps to $\simeq 50\%$ coverage for $r_{\text{NME}} = 1.5$ for both cases of $\alpha_{31} = 0$ and π . It is also notable that in the inverted mass hierarchy case the sensitivity region reaches to the range

⁶ We have examined the similar f_{CPX} plots for several input values of α_{31} , 0, $\pi/4$, $\pi/2$, and π . The exercise revealed that for $\alpha_{21} \gtrsim 0.6\pi$, the best and the worst sensitivities are obtained at $\alpha_{31} = \pi$ and $\alpha_{31} = 0$, respectively, the cases used in Fig. 7. For $\alpha_{21} \lesssim 0.6\pi$, this behaviour become opposite, leading to the worst and best sensitivity at $\alpha_{31} = \pi$ and $\alpha_{31} = 0$, respectively,

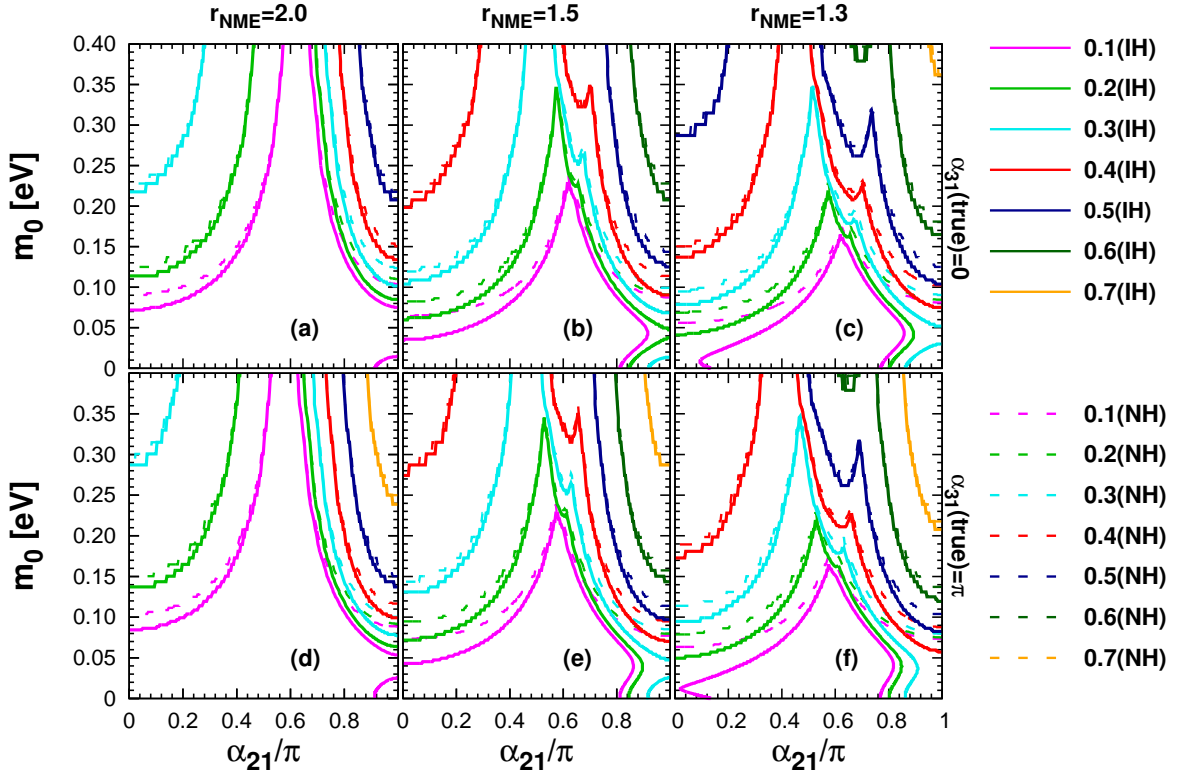


FIG. 7: Contours of CP exclusion fraction determined at 2σ CL (1 DOF) projected into the plane of the true values of α_{21}/π and the lightest neutrino mass m_0 for the case where $r_{\text{NME}} = 2$ (left panels), 1.5 (middle panels) and 1.3 (right panels) and the true value of $\alpha_{31} = 0$ (upper panels) and π (lower panels). The case for the inverted (IH) and normal (NH) mass hierarchy are shown, respectively, by the solid and dashed curves, from 0.1 to 0.7 with the step size of 0.1

$0 \text{ eV} \leq m_0 \lesssim 0.05 \text{ eV}$, though only up to $f_{\text{CPX}} \simeq 0.1$ – 0.2 , the tendency more and more visible for smaller values of r_{NME} . Therefore, reducing the NME uncertainty is of crucial importance to have severer constraints (or to observe) the Majorana phase.

Though it is encouraging to see some sensitivities to the Majorana phase thanks to precision measurement of Σ and $0\nu\beta\beta$ decay rate, we must remark that it is still at a relatively low level. For example, in the case of $m_0 \simeq 0.1 \text{ eV}$, which is preferred by some cosmological analyses, the sensitivity to α_{21} is up to $f_{\text{CPX}} \simeq 0.1$ – 0.3 level even in the most optimistic case of $r_{\text{NME}} = 1.3$ except for the region close to $\alpha_{21} = \pi$ (see panels (c) and (f) of Fig. 7).

Therefore, we examine below two possibilities toward further improvement of the sensitivity to α_{21} : (1) Higher precision measurement of neutrino masses in Cosmology as good as $\sigma_\Sigma = 0.02 \text{ eV}$, and (2) Revolutionary new technology of computing the NME of $0\nu\beta\beta$ decay which could lead to uncertainty of the level $r_{\text{NME}} = 1.1$. As mentioned before, once the positive signal of $0\nu\beta\beta$ will be observed by using different isotopes, we hope that theoretical NME calculations can be “calibrated” to some extent using the real data. (We tentatively assume that 10% level uncertainty is unavoidable.) It is discussed that the former is within reach in the light of future cosmological observation as mentioned in section II B [65–67]. On the other hand, it remains to be seen how (2) can be realized.

We first consider the possibility (1). In the upper panels in Fig. 8 we show the same plots as shown in the upper panels of Fig. 7, the case where the true value of $\alpha_{21} = 0$, but generated only by changing the value of σ_Σ from 0.05 eV to 0.02 eV to compute f_{CPX} . By comparing results shown in the upper panels of Fig. 8 to the case of $\sigma_\Sigma = 0.05 \text{ eV}$ shown in upper panels of Fig. 7, at 2σ CL, in the parameter regions corresponding to $\alpha_{21} \lesssim 0.6\pi$, the improvement (increase of f_{CPX}) with $\sigma_\Sigma = 0.02 \text{ eV}$ is not so large, typically less than 0.1. However, for $\alpha_{21} \gtrsim 0.6\pi$, we observe that there are some regions, in $m_0 \lesssim 0.2 \text{ eV}$, where the improvement is more significant, leading to $\Delta f_{\text{CPX}}(\Sigma) \equiv f_{\text{CPX}}(\Sigma = 0.02 \text{ eV}) - f_{\text{CPX}}(\Sigma = 0.05 \text{ eV}) \sim 0.1$ – 0.3 . For instance, at around $m_0 \simeq 0.1 \text{ eV}$ and $\alpha_{21} \simeq 0.8\pi$, for $r_{\text{NME}} = 1.5$, $\Delta f_{\text{CPX}}(\Sigma)$ is ~ 0.2 or so (see Fig. 8(e) and text below).

It is not so easy to see clearly, just by comparing by eyes the upper panels of Figs. 7 and 8, in which parameter regions in the $\alpha_{21} - m_0$ plane the impact of reducing the error for the determination of Σ is large, and how large is the effect. Therefore, we show in the lower panels of Fig. 8 the iso-contours of $\Delta f_{\text{CPX}}(\Sigma)$, the difference between the results shown in the upper panels of Figs. 7 and 8, defined in the previous paragraph. The panels (d), (e) and (f) in Fig. 8 are for $r_{\text{NME}} = 2.0$, 1.5 and 1.3, respectively. They illuminate more clearly how much the sensitivity improves

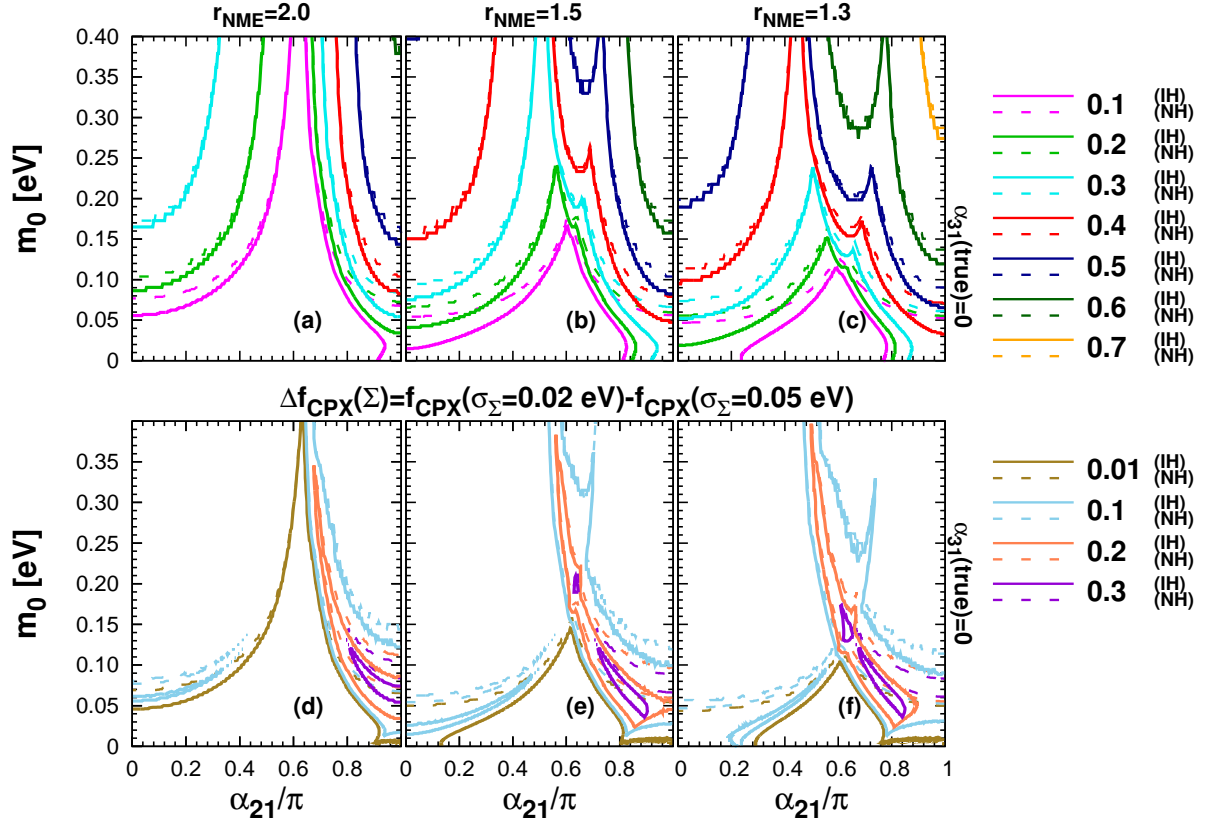


FIG. 8: Upper panels in (a), (b) and (c): same as in the upper panels of Fig. 7, iso-contours of f_{CPX} determined at 2σ CL, but with the value of $\sigma_\Sigma = 0.02$ eV keeping all the other conditions the same as in Fig. 7. Lower panels in (d), (e) and (f): iso-contours of $\Delta f_{\text{CPX}}(\Sigma) \equiv f_{\text{CPX}}(\Sigma = 0.02 \text{ eV}) - f_{\text{CPX}}(\Sigma = 0.05 \text{ eV})$, the difference of the results shown in the upper panels of Figs. 8 and 7.

with reduced σ_Σ (larger $\Delta f_{\text{CPX}}(\Sigma) > 0$ implies larger improvement). We confirm that for $\alpha_{21} \lesssim (0.5-0.6)\pi$, the impact of reducing σ_Σ is rather small, $\Delta f_{\text{CPX}}(\Sigma) \lesssim 0.1$, whereas for $\alpha_{21} \gtrsim (0.5-0.6)\pi$, there are some regions where the improvement is relatively large, or $\Delta f_{\text{CPX}}(\Sigma)$ is larger than 0.2 (inside the regions delimited by the solid orange curves in the lower panels, (d), (e) and (f) of Fig. 8).

Finally, let us make a comparison, at 3σ CL, by changing σ_Σ from 0.05 eV to 0.02 eV and/or r_{NME} from 1.3 to the extreme value of 1.1, the possibility (2) mentioned above. In Fig. 9 we show the cases of $(\sigma_\Sigma, r_{\text{NME}}) = (0.05 \text{ eV}, 1.3)$, $(0.05 \text{ eV}, 1.1)$, $(0.02 \text{ eV}, 1.3)$ and $(0.02 \text{ eV}, 1.1)$, respectively, in the panels (a), (b), (d) and (e). As done for Fig. 8, we only consider the case of the true value of $\alpha_{31} = 0$ since the overall behaviours of these plots does not depend so much on the assumed value of $\alpha_{31} = 0$. Since we are considering the extreme values of σ_Σ and r_{NME} we show our results at 3σ CL.

The panels (g) and (h) are to show the difference of f_{CPX} obtained when σ_Σ , the uncertainty in Σ , get decreased from 0.05 eV to 0.02 eV, keeping r_{NME} fixed; Exhibited in the panels (g) and (h) are the iso-contours of $\Delta f_{\text{CPX}}(\Sigma)$ for the cases with $r_{\text{NME}} = 1.3$ and 1.1, respectively. Whereas the panels (c) (the case of $\sigma_\Sigma = 0.05$ eV) and (f) ($\sigma_\Sigma = 0.02$ eV) of Fig. 9 are to show the difference of f_{CPX} when $r_{\text{NME}} = 1.3$ is varied to 1.1 by keeping σ_Σ fixed, $\Delta f_{\text{CPX}}(r_{\text{NME}}) \equiv f_{\text{CPX}}(r_{\text{NME}} = 1.1) - f_{\text{CPX}}(r_{\text{NME}} = 1.3)$, an ultimate improvement of the NME calculation. Finally, in the panel (i), the iso-contours of $\Delta f_{\text{CPX}}(\Sigma, r_{\text{NME}}) \equiv f_{\text{CPX}}(\sigma_\Sigma = 0.02 \text{ eV}, r_{\text{NME}} = 1.1) - f_{\text{CPX}}(\sigma_\Sigma = 0.05 \text{ eV}, r_{\text{NME}} = 1.3)$ are displayed to illuminate the impact of reducing both σ_Σ and r_{NME} simultaneously.

We first note that, by looking the plots which show the iso-contours of $\Delta f_{\text{CPX}}(\Sigma)$ or $\Delta f_{\text{CPX}}(r_{\text{NME}})$ in the panels (c), (f), (g), (h) and (i) of Fig. 9, the qualitative behaviours of these plots appear to be similar as the one shown in the lower panels (d), (e) and (f) of Fig. 8. More precisely, we observe that for $\alpha_{21} \lesssim 0.4\pi$ there is no significant improvement of the sensitivity by reducing σ_Σ and/or r_{NME} . Even for $\alpha_{21} \gtrsim 0.4\pi$ the significant improvement corresponding $\Delta f_{\text{CPX}} \geq 0.3$ (delimited by the solid magenta curves in (c), (f), (g), (h) and (i)) are obtained in some limited parameter regions. By comparing (c) versus (g) or (f) versus (h), we observe that the impact of reducing σ_Σ from 0.05 eV to 0.02 eV is larger than that of reducing r_{NME} from 1.3 to 1.1 as we can see in (g) and (h) there are more larger regions corresponding $\Delta f_{\text{CPX}} \geq 0.3$ (delimited by the solid purple curves) than in (c) and (f). By looking at

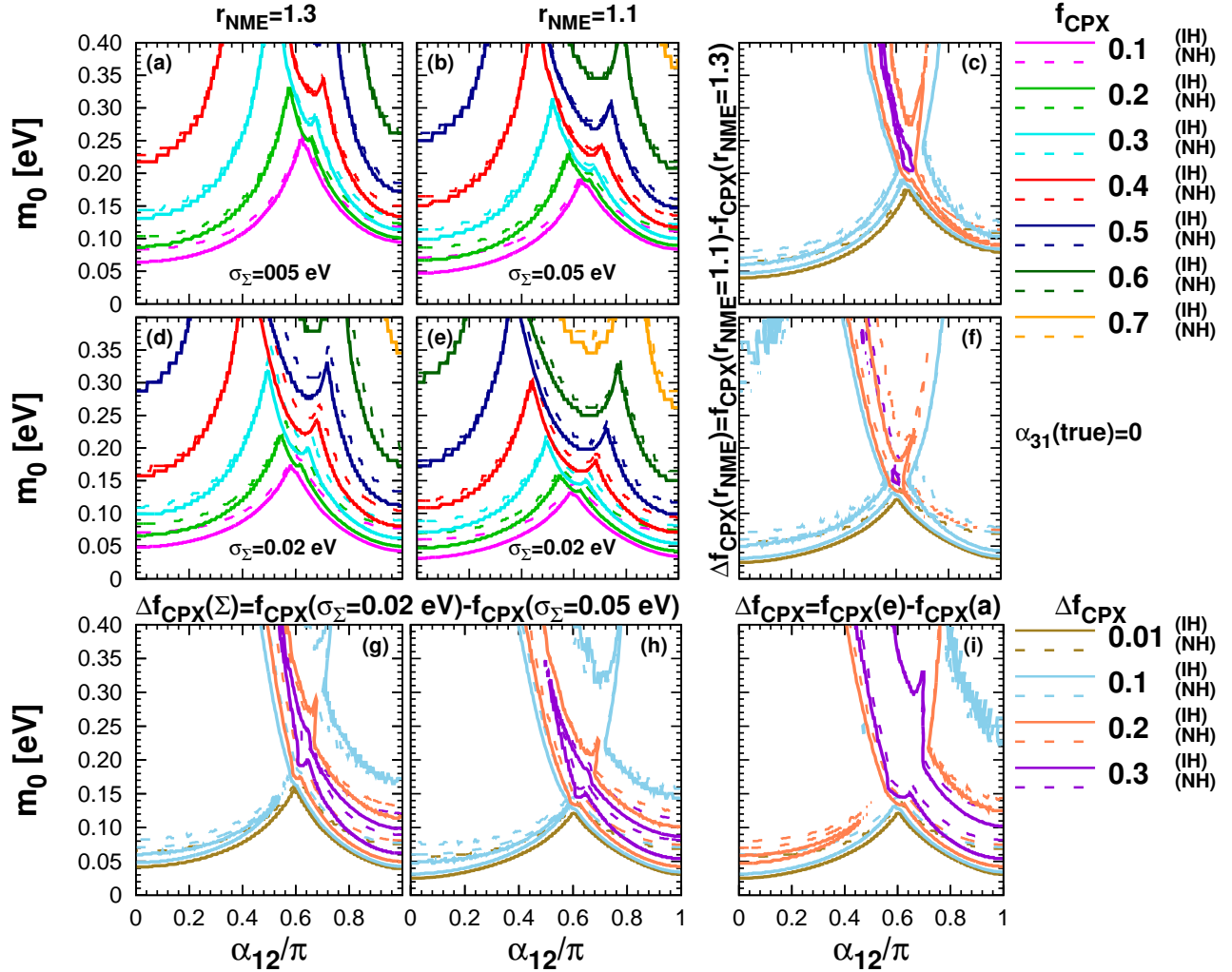


FIG. 9: In (a), (b), (d), (e) similar plots as in Fig. 7 and upper panels of Fig. 8 but f_{CPX} computed at 3σ and for the cases where true value of $(\sigma_\Sigma, r_{\text{NME}}) =$ (a) (0.05 eV, 1.3), (b) (0.05 eV, 1.1), (d) (0.02 eV, 1.3) and (e) (0.02 eV, 1.1) are shown. In (c) and (f), we show, respectively, for $\sigma_\Sigma = 0.05$ eV and 0.02 eV, the iso-contours of $\Delta f_{\text{CPX}}(r_{\text{NME}}) \equiv f_{\text{CPX}}(r_{\text{NME}} = 1.1) - f_{\text{CPX}}(r_{\text{NME}} = 1.3)$ whereas in (g) and (h), we show, respectively, for $r_{\text{NME}} = 1.3$ and 1.1, the iso-contours of $\Delta f_{\text{CPX}}(\Sigma) \equiv f_{\text{CPX}}(\sigma_\Sigma = 0.02 \text{ eV}) - f_{\text{CPX}}(\sigma_\Sigma = 0.05 \text{ eV})$. In (i) we show the iso-contours of $\Delta f_{\text{CPX}}(\Sigma, r_{\text{NME}}) \equiv f_{\text{CPX}}(\sigma_\Sigma = 0.02 \text{ eV}, r_{\text{NME}} = 1.1) - f_{\text{CPX}}(\sigma_\Sigma = 0.05 \text{ eV}, r_{\text{NME}} = 1.3)$.

(i) we can see that the simultaneous reduction of both σ_Σ and r_{NME} increase considerably the regions corresponding to $\Delta f_{\text{CPX}} \geq 0.3$.

VIII. IS IT POSSIBLE TO CONSTRAIN THE NUCLEAR MATRIX ELEMENT?

Finally, let us consider the possibility to constrain the nuclear matrix element only from the experiments. So far we have been assuming that the NME is restricted to some range since, in principle, it can be computed theoretically. The question we ask in this section is: “Is it possible to obtain some non-trivial constraint on the NME just by the experimental consistency even though we let the NME vary completely freely in the fit?” This is of course under the assumption of neutrino mass mechanism of $0\nu\beta\beta$ decay.

In order to answer this question, we have repeated the same analyses but without imposing any condition on the NME uncertainty parameter $\xi \equiv \mathcal{M}_0^{(0\nu)}/\mathcal{M}^{(0\nu)}$ where $\mathcal{M}_0^{(0\nu)}$ is the reference NME value defined in Eq. (25) in section IV B, used to translate the measured half life to $m_{0\nu\beta\beta}$ and $\mathcal{M}^{(0\nu)}$ is the true NME value which is now assumed to be completely unknown.

In Fig. 10 we show the similar results shown in Figs. 2 and 3 but for the NME uncertainty parameter ξ , namely, $\Delta\chi^2$ as a function of ξ for different true values of $\alpha_{21} = 0, \pi/4, \pi/2$ and π for the case of the inverted mass hierarchy

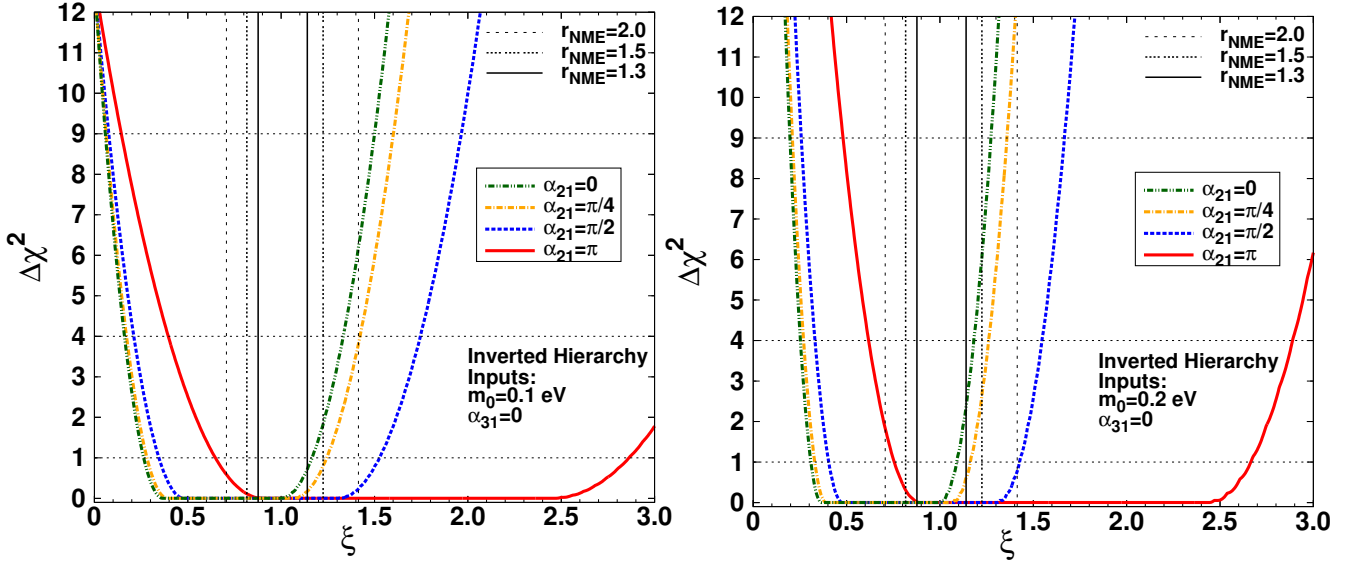


FIG. 10: $\Delta\chi^2$ is plotted as a function of the fitted parameter, $\xi \equiv \mathcal{M}_0^{(0\nu)}/\mathcal{M}^{(0\nu)}$ for different true values of $\alpha_{21} = 0, \pi/4, \pi/2$ and π for the case of the inverted mass hierarchy with $m_0 = 0.1$ eV (left panel) and 0.2 eV (right panel) where the other parameters, m_0 , α_{21} and α_{31} are marginalized. The ranges of ξ corresponding to the cases of $r_{\text{NME}} = 2.0, 1.5$ and 1.3 are also shown, respectively, by the black-dashed, black-dotted and black-solid lines in the same plots.

with $m_0 = 0.1$ eV (left panel) and 0.2 eV (right panel). The ranges of ξ corresponding to the cases of $r_{\text{NME}} = 2.0, 1.5$ and 1.3 are also shown, respectively by the black dashed, dotted and solid lines in the same plots. We only show the case of the inverted mass hierarchy since that results for the normal hierarchy case is similar. We note that the case of the inverted mass hierarchy can constrain somewhat better the NME uncertainty parameter ξ than the case of the normal hierarchy (not shown). From this plot, we can see that in some regions, $\alpha_{21} \lesssim 0.5\pi$ or around π , it is possible to restrict (although not so severely) the possible range of the NME only from the consistency of the results of the experiments.

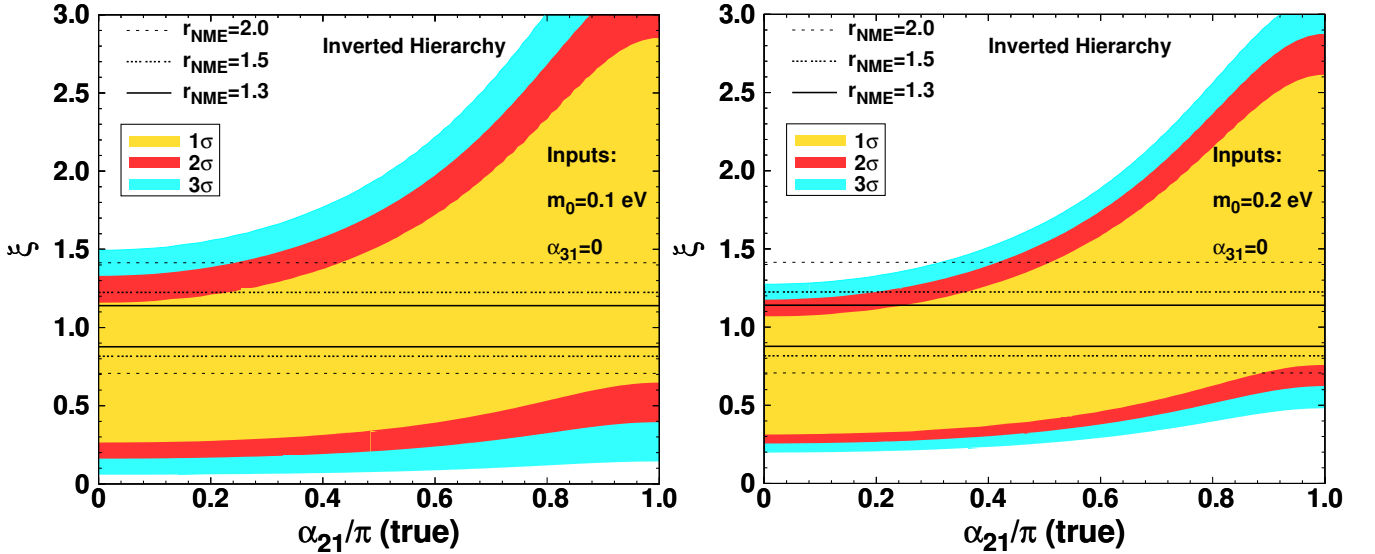


FIG. 11: Ranges of the fitted value of ξ allowed at 1, 2 and 3 σ CL, for 1 DOF, indicated, respectively, by the colored regions of yellow, red and light blue, as a function of the true value of α_{21} for $\alpha_{31}(\text{true}) = 0$, $m_0(\text{true}) = 0.1$ eV (left panel) and 0.2 eV (right panel) for the case of the inverted mass hierarchy. The ranges of ξ corresponding to the cases of $r_{\text{NME}} = 2.0, 1.5$ and 1.3 are also shown, respectively by the black dashed, dotted and solid lines.

In Fig. 11 we show the ranges of the fitted value of ξ allowed at 1, 2 and 3 σ CL, for 1 DOF, indicated, respectively, by filled colors of yellow, red and light blue, as a function of the true values of α_{21} for the case of $\alpha_{31}(\text{true}) = 0$, $m_0(\text{true}) = 0.1$ eV (left panel) and 0.2 eV (right panel) for the case of the inverted mass hierarchy. From this plot,

if the true value of $\alpha_{21} \sim 0$, we can constrain better the upper value of ξ whereas if $\alpha_{21} \sim \pi$ we can constrain better the lower limit of ξ though the restricting power is not so strong.

To summarize: Assuming the standard three flavor scheme and standard mechanism of light neutrino exchange for $0\nu\beta\beta$ decay, it is possible to perform a consistency check of the NME calculation and one may be able to exclude some version of the NME obtained. If good fit is obtained only for some value of ξ well beyond the range expected from the theoretical uncertainty, this could imply the presence of new physics such as, for example, the sterile neutrino contribution. See e.g, Refs. [82–84] where the impact of the sterile neutrinos on double beta decay was studied.

IX. CONCLUSIONS AND DISCUSSION

In this paper, we have studied how and to what extent the Majorana phases can be constrained under the assumption of highly accurate measurement of $0\nu\beta\beta$ decay rate and stringent constraint on sum of neutrino masses by cosmological observation. The remarkable feature of our results is that the synergy between cosmology and double beta decay experiments in constraining the Majorana phase is quite visible; We have demonstrated that it is possible to obtain highly non-trivial constraints on the Majorana phase, if accurate measurement of Σ is added, even if double beta decay experiment alone can not say anything about the Majorana phase. Notice that double beta decay experiment by itself cannot place any useful constraints on the Majorana phase in our current setting, not because they suffer from the NME (Nuclear Matrix Element) uncertainty (which of course makes it worse if it exists), but because they lack independent key information of the absolute neutrino mass scale in itself.

The general tendency of the sensitivity to the Majorana phases are as follows:

- Dependence of $m_{0\nu\beta\beta}$ on α_{31} , one of the two Majorana phases, is very weak due to the suppression by s_{13}^2 . Hence, little sensitivity can be expected for α_{31} , and the sensitivity to α_{21} depend on α_{31} but only very weakly.
- The regions of the best and the worst sensitivities to α_{21} are located at around the true values $\alpha_{21} \simeq 0$ or π , and at $\alpha_{21} \simeq 2\pi/3$, respectively, in agreement with our analytic estimate in Sec. IIIB.
- For both mass hierarchies and within any uncertainties of the NME used, the better sensitivity to the CP phase α_{21} is obtained for larger value of m_0 , apart from minor exception of region $m_0 \lesssim 0.05$ eV, mostly in the horizontal branch in Fig. 1 for the inverted mass hierarchy.

We took as the reference set up that the effective masses observed in $0\nu\beta\beta$ and β decay experiments can be measured with the uncertainty of 0.01 eV and 0.06 eV, respectively, whereas the sum of neutrino masses Σ can be determined with the uncertainty of 0.05 eV by cosmological observation. We have assumed the uncertainty r_{NME} , defined as the ratio of the maximum and minimum values of the theoretically expected NME values, between factor of 1.3 – 2.0 and treated it in a different way from these experimental errors (which is similar to the treatment of flux normalization uncertainty). To show the dependence of these assumed errors on sensitivity to Majorana phase, we have examined in the last part of our analysis, the case with more aggressive errors, 0.02 eV for the error of Σ and $r_{\text{NME}} = 1.1$ for the NME uncertainty. We note here that we took a fixed error (0.01 eV) for $m_{0\nu\beta\beta}$ based on the discussion given in Appendix A. If a percentage error for $m_{0\nu\beta\beta}$ is to be assumed, the sensitivity to α_{21} in region $m_0 \lesssim 0.05$ eV would be greatly enhanced.

To display the sensitivities to the Majorana phase quantitatively we have used the two measures, (1) the conventional allowed region plots, and (2) CP exclusion fraction f_{CPX} , a fraction of the CP phase space that can be excluded for a given set of input parameters. We believe that f_{CPX} is a useful global measure, as the CP fraction widely used in the sensitivity studies for the long baseline neutrino oscillation experiments is, but in a different way. That is, f_{CPX} is better suited to reveal (relatively poor) sensitivities in the early era of the search for the CP phase effect, as discussed in Ref. [48]. Since measuring the Majorana phase is very challenging in any means, we believe that even the partial exclusion of its possible range is quite useful.

We have shown with our reference setup and $r_{\text{NME}} = 1.5$ that α_{21} can be constrained by excluding $\simeq 10 - 40\%$ of the phase space of α_{21} at 2σ CL for the lowest neutrino mass of 0.1 eV for both mass hierarchies. Even if we use 0.02 eV for the error of Σ the excluding fraction does not change much, and is $\simeq 10 - 50\%$. Fortunately, the f_{CPX} contours are rather stiff against change in CL from 2σ to 3σ so that they stay more or less the same, as shown in Fig. 8, indicating robust nature of sensitivity to the Majorana phase resistant to high CL demand. We also should note that the sensitivity to α_{21} becomes significantly better when the uncertainty of the nuclear matrix element (r_{NME}) is reduced from the factor 2 to 1.5, independent of the assumed mass hierarchy and value of α_{31} .

It is only recently that such a discussion started to obtain real perspective because cosmology entered into the precision era, as demonstrated most notably an epoch making precision measurement achieved by Planck. Yet, the accuracy of measurement of the sum of neutrino masses which warrants reasonably strong restriction to the Majorana phase is rather demanding, $\Sigma \simeq 0.01 - 0.02$ eV, which probably requires the Euclid satellite as well as the next

generation galaxy surveys, in addition to the better understanding of the different systematics exist in the different set of the cosmological data. Of course, it also requires accurate measurement of lifetime of $0\nu\beta\beta$ decay in a ton scale experiment with very low background, which would allow uncertainty in measurement of $m_{0\nu\beta\beta}$ as small as $\simeq 0.01$ eV.

One may argue that too much relying on cosmological observation in determining Σ is dangerous because, neutrinos being a minor player in the universe, its precise determination is possible only in a model dependent way. Though it is a valid point we must bear in mind that future precision observation itself offers an even more stringent test of the Λ CDM paradigm. Therefore, we have implicitly assumed as a prerequisite of the analysis that the paradigm (or even an alternative cosmological model) will be established in a sufficient robustness to allow reliable measurement of the neutrino component. The discussion in this paper would serve as a prototype of the similar analysis after we have acquired the established standard cosmological model.

Finally, we also studied the possibility to constrain the nuclear matrix element only from the consistency of the experimental results by varying its value completely freely. We found that in some limited situation where $\alpha_{21} \simeq 0$ or π , it is possible to obtain non-trivial constraint on the nuclear matrix element, which can be used as a consistency check of its theoretical calculation.

Appendix A: Estimation of the sensitivity to $m_{0\nu\beta\beta}$ in neutrinoless double beta decay experiment

Let us estimate the expected precision on $m_{0\nu\beta\beta}$ to be observed in the $0\nu\beta\beta$ decay experiment. See Refs. [33–35, 76–78] for more detailed discussions on the experimental sensitivities. Here we ignore the theoretical uncertainty of the nuclear matrix element, $\mathcal{M}^{(0\nu)}$, which will be taken care of in a different way as discussed in section IV.

From Eq. (1) we obtain the following expression for the effective mass,

$$m_{0\nu\beta\beta} = \frac{m_e}{\sqrt{T_{1/2}^{0\nu} G_{0\nu} |\mathcal{M}^{(0\nu)}|^2}}. \quad (\text{A1})$$

The expected number of $0\nu\beta\beta$ decays (signal) to be observed in the experiment, $N_{0\nu\beta\beta}$, is given by

$$N_{0\nu\beta\beta} = \varepsilon_{\text{det}} \frac{m_X N_A}{W_X} \left[1 - \exp\left(-\frac{t_{\text{exp}} \ln 2}{T_{1/2}^{0\nu}}\right) \right] \simeq \frac{\varepsilon_{\text{det}} N_A m_X t_{\text{exp}} \ln 2}{W_X T_{1/2}^{0\nu}} \quad (\text{A2})$$

where ε_{det} is the detection efficiency, m_X and W_X are respectively, the total mass and the molecular weight of the isotope X to be used in the double beta decay experiment, N_A is the Avgadro's number and t_{exp} is the exposure time, assumed to be much smaller than $T_{1/2}^{0\nu}$.

On the other hand, the expected number of the background events can be expressed as,

$$N_{\text{BG}} = b \Delta E m_X t_{\text{exp}}, \quad (\text{A3})$$

where b is the number of background counts usually measured in $\text{keV}^{-1} \text{ kg}^{-1} \text{ yr}^{-1}$, ΔE is the energy window (\sim energy resolution) given in keV around the $0\nu\beta\beta$ peak, both of which depend on the experimental set up we consider.

Roughly speaking, the expected sensitivity of the double beta decay experiment for the half life time is obtained when $N_{0\nu\beta\beta} \sim \sqrt{N_{\text{BG}}}$, which implies that

$$T_{1/2}^{0\nu} \sim \frac{\varepsilon_{\text{det}} N_A m_X t_{\text{exp}} \ln 2}{W_X \sqrt{b \Delta E m_X t_{\text{exp}}}} = \frac{\varepsilon_{\text{det}} N_A \ln 2}{W_X} \sqrt{\frac{m_X t_{\text{exp}}}{b \Delta E}}. \quad (\text{A4})$$

This can be translated in terms of the minimum possible observable value of $m_{0\nu\beta\beta}^{\text{min}}$ as [79],

$$m_{0\nu\beta\beta}^{\text{min}} \sim \frac{m_e}{\sqrt{G_{0\nu} |\mathcal{M}^{(0\nu)}|^2 \ln 2}} \left[\frac{W_X}{\varepsilon_{\text{det}} N_A} \right]^{\frac{1}{2}} \left[\frac{b \Delta E}{m_X t_{\text{exp}}} \right]^{\frac{1}{4}}. \quad (\text{A5})$$

If we consider, for example, the isotopes of ^{76}Ge and ^{136}Xe , by using the typical values for $G_{0\nu}$ and $\mathcal{M}^{(0\nu)}$ found, e.g., in Ref. [35], and typical background rate and energy resolutions, for ^{76}Ge (by using $G_{0\nu} = 2.36 \times 10^{-15} \text{ yr}^{-1}$ [54]) we obtain,

$$m_{0\nu\beta\beta}^{\min} \sim 0.12 \left[\frac{5.0}{\mathcal{M}^{(0\nu)}} \right] \left[\frac{b}{0.01 \text{ keV} \cdot \text{kg} \cdot \text{yr}} \right]^{\frac{1}{4}} \left[\frac{\Delta E}{3.5 \text{ keV}} \right]^{\frac{1}{4}} \left[\frac{100 \text{ kg} \cdot \text{yr}}{\varepsilon_{\text{det}}^2 \cdot m_{\text{Ge}} \cdot t_{\text{exp}}} \right]^{\frac{1}{4}} \text{ eV}, \quad (\text{A6})$$

whereas for ^{136}Xe (by using $G_{0\nu} = 14.58 \times 10^{-15} \text{ yr}^{-1}$ [54]) we obtain,

$$m_{0\nu\beta\beta}^{\min} \sim 0.24 \left[\frac{3.0}{\mathcal{M}^{(0\nu)}} \right] \left[\frac{b}{0.01 \text{ keV} \cdot \text{kg} \cdot \text{yr}} \right]^{\frac{1}{4}} \left[\frac{\Delta E}{100 \text{ keV}} \right]^{\frac{1}{4}} \left[\frac{100 \text{ kg} \cdot \text{yr}}{\varepsilon_{\text{det}}^2 \cdot m_{\text{Xe}} \cdot t_{\text{exp}}} \right]^{\frac{1}{4}} \text{ eV}, \quad (\text{A7})$$

where m_{Ge} (m_{Xe}) is the total mass of the isotope of ^{76}Ge (^{136}Xe) to be used in the double beta decay experiments. If $0\nu\beta\beta$ decay will be actually observed, at first approximation, we assume that these values could be roughly corresponds to the uncertainty on the measurement of $m_{0\nu\beta\beta}$, or $\sigma_{0\nu\beta\beta}$.

As we can see, as the sensitivity improves only as the one of the fourth power of the size of the experiment, background and energy resolution, it is seems not so easy to improve the sensitivity and looks quite difficult to reach the level of $\sigma_{0\nu\beta\beta} \sim O(0.01) \text{ eV}$, even if we consider ~ 1 ton scale experiment. Therefore, it would be necessary to realize the background free or very low background experiment to achieve such a level (see below).

Next let us consider the case that the background rate b is so low that N_{BG} in Eq. (A3) is negligible, or namely, *zero background* experiment [35]. In this case, from the number of observed events, $N_{0\nu\beta\beta}$, the half life time can be estimated as

$$T_{1/2}^{0\nu} = \frac{\varepsilon_{\text{det}} n_X t_{\text{exp}} \ln 2}{N_{0\nu\beta\beta}}, \quad (\text{A8})$$

and its uncertainty is estimated as

$$\delta(T_{1/2}^{0\nu}) \sim T_{1/2}^{0\nu} \frac{\delta(N_{0\nu\beta\beta})}{N_{0\nu\beta\beta}} \sim T_{1/2}^{0\nu} \frac{1}{\sqrt{N_{0\nu\beta\beta}}}. \quad (\text{A9})$$

Then from Eqs. (A1) and (A9) we obtain

$$\sigma_{0\nu\beta\beta} \equiv \delta(m_{0\nu\beta\beta}) \sim \frac{1}{2} m_{0\nu\beta\beta}^{(0)} \frac{\delta(T_{1/2}^{0\nu})}{T_{1/2}^{0\nu}} \sim \frac{1}{2} m_{0\nu\beta\beta}^{(0)} \frac{1}{\sqrt{N_{0\nu\beta\beta}}} \sim \frac{m_e}{2\sqrt{G_{0\nu}} |\mathcal{M}^{(0\nu)}|^2 \varepsilon_{\text{det}} (m_X N_A / W_X) t_{\text{exp}} \ln 2}. \quad (\text{A10})$$

We note that the result does not depend on the life time, and the uncertainty can be arbitrarily small as we increase the product of the source mass and exposure time of the experiment by considering only the statistical error, until the point that the background could no longer be neglected.

By using the same numbers for $G_{0\nu}$ and $\mathcal{M}^{(0\nu)}$ we used to obtain $m_{0\nu\beta\beta}^{\min}$ in Eqs. (A6) and (A7) and), for ^{76}Ge , we obtain,

$$\sigma_{0\nu\beta\beta} \sim 0.06 \left[\frac{100 \text{ kg} \cdot \text{yr}}{\varepsilon_{\text{det}} \cdot m_{\text{Ge}} \cdot t_{\text{exp}}} \right]^{\frac{1}{2}} \left[\frac{5.0}{\mathcal{M}^{(0\nu)}} \right] \text{ eV}, \quad (\text{A11})$$

whereas for ^{136}Xe , we obtain,

$$\sigma_{0\nu\beta\beta} \sim 0.04 \left[\frac{100 \text{ kg} \cdot \text{yr}}{\varepsilon_{\text{det}} \cdot m_{\text{Xe}} \cdot t_{\text{exp}}} \right]^{\frac{1}{2}} \left[\frac{3.0}{\mathcal{M}^{(0\nu)}} \right] \text{ eV}. \quad (\text{A12})$$

We expect that these values should coincide roughly with the minimum possible observable values (or sensitivities) of the experiments, or $\sigma_{0\nu\beta\beta} \sim m_{0\nu\beta\beta}^{\min}$. Therefore, as long as the background is neglected, by considering the ~ 1 ton size experiment, it seems possible to reach the level of $\sigma_{0\nu\beta\beta} \sim O(0.01) \text{ eV}$. In this work, for definiteness and simplicity, we assume that $m_{0\nu\beta\beta}$ can be determined with an accuracy of 0.01 eV for a given reference value of the NME. See the section IV B how to take into account the NME uncertainty. We note, however, that in reality, the fate of the background would not be so simple to allow analytic treatment as ours. Therefore, most probably, one needs to perform detailed numerical simulations to reliably estimate the experimental uncertainties in measurement of the double beta decay lifetime.

Acknowledgments

The authors thank Kunio Inoue for informative correspondences on neutrinoless double beta decay experiment and Shun Saito on the cosmological determination of neutrino masses. H.M. is grateful to CNPq for support for his visit to the Departamento de Física, Pontifícia Universidade Católica do Rio de Janeiro. He thanks Universidade de São Paulo for the great opportunity of stay as Pesquisador Visitante Internacional. He is also partially supported by KAKENHI received through Tokyo Metropolitan University, Grant-in-Aid for Scientific Research No. 23540315, Japan Society for the Promotion of Science. H.N. thanks the hospitality of Osamu Yasuda and Omar Miranda, respectively, at the Department of Physics of Tokyo Metropolitan University and of CINVESTAV-IPN where the final part of this manuscript was done. This work was supported by Fundação de Amparo à Pesquisa do Estado do Rio de Janeiro (FAPERJ) and Conselho Nacional de Ciência e Tecnologia (CNPq).

-
- [1] Z. Maki, M. Nakagawa and S. Sakata, Prog. Theor. Phys. **28**, 870 (1962).
 - [2] T. Kajita, Adv. High Energy Phys. **2012**, 504715 (2012).
 - [3] A. B. McDonald, New J. Phys. **6**, 121 (2004) [arXiv:astro-ph/0406253].
 - [4] K. Inoue, New J. Phys. **6**, 147 (2004).
 - [5] M. Kobayashi and T. Maskawa, Prog. Theor. Phys. **49**, 652 (1973).
 - [6] J. Schechter and J. W. F. Valle, Phys. Rev. D **22**, 2227 (1980).
 - [7] S. M. Bilenky, J. Hosek and S. T. Petcov, Phys. Lett. B **94**, 495 (1980).
 - [8] M. Doi, T. Kotani, H. Nishiura, K. Okuda and E. Takasugi, Phys. Lett. B **102**, 323 (1981).
 - [9] M. Fukugita and T. Yanagida, Phys. Lett. B **174**, 45, (1986).
 - [10] H. Minakata and O. Yasuda, Phys. Rev. D **56**, 1692 (1997) [hep-ph/9609276].
 - [11] S. M. Bilenky, S. Pascoli and S. T. Petcov, Phys. Rev. D **64**, 053010 (2001) [hep-ph/0102265].
 - [12] M. Czakon, J. Gluza, J. Studnik and M. Zralek, Phys. Rev. D **65**, 053008 (2002) [hep-ph/0110166].
 - [13] S. Pascoli, S. T. Petcov and L. Wolfenstein, Phys. Lett. B **524**, 319 (2002) [hep-ph/0110287].
 - [14] V. Barger, S. L. Glashow, P. Langacker and D. Marfatia, Phys. Lett. B **540**, 247 (2002) [hep-ph/0205290].
 - [15] H. Nunokawa, W. J. C. Teves and R. Zukanovich Funchal, Phys. Rev. D **66**, 093010 (2002) [hep-ph/0206137].
 - [16] S. Pascoli, S. T. Petcov and W. Rodejohann, Phys. Lett. B **549**, 177 (2002) [hep-ph/0209059].
 - [17] F. Deppisch, H. Pas and J. Suhonen, Phys. Rev. D **72**, 033012 (2005) [hep-ph/0409306].
 - [18] A. Joniec and M. Zralek, Phys. Rev. D **73**, 033001 (2006) [hep-ph/0411070].
 - [19] S. Pascoli, S. T. Petcov and T. Schwetz, Nucl. Phys. B **734**, 24 (2006) [hep-ph/0505226].
 - [20] S. Choubey and W. Rodejohann, Phys. Rev. D **72**, 033016 (2005) [hep-ph/0506102].
 - [21] F. Simkovic, S. M. Bilenky, A. Faessler and T. Gutsche, Phys. Rev. D **87**, 073002 (2013) [arXiv:1210.1306 [hep-ph]].
 - [22] P. A. R. Ade *et al.* [Planck Collaboration], arXiv:1303.5076 [astro-ph.CO].
 - [23] K. N. Abazajian, E. Calabrese, A. Cooray, F. De Bernardis, S. Dodelson, A. Friedland, G. M. Fuller and S. Hannestad *et al.*, Astropart. Phys. **35**, 177 (2011) [arXiv:1103.5083 [astro-ph.CO]].
 - [24] R. A. Battye and A. Moss, arXiv:1308.5870 [astro-ph.CO].
 - [25] M. Auger *et al.* [EXO Collaboration], Phys. Rev. Lett. **109**, 032505 (2012) [arXiv:1205.5608 [hep-ex]].
 - [26] A. Gando *et al.* [KamLAND-Zen Collaboration], Phys. Rev. Lett. **110**, 062502 (2013) [arXiv:1211.3863 [hep-ex]].
 - [27] M. Agostini *et al.* [GERDA Collaboration], Phys. Rev. Lett. **111**, 122503 (2013) [arXiv:1307.4720 [nucl-ex]].
 - [28] C. Arnaboldi *et al.* [CUORE Collaboration], Nucl. Instrum. Meth. A **518**, 775 (2004) [hep-ex/0212053].
 - [29] J. Hartnell [SNO+ Collaboration], J. Phys. Conf. Ser. **375**, 042015 (2012) [arXiv:1201.6169 [physics.ins-det]].
 - [30] R. Gaitskell *et al.* [Majorana Collaboration], nucl-ex/0311013.
 - [31] R. Arnold *et al.* [SuperNEMO Collaboration], Eur. Phys. J. C **70**, 927 (2010) [arXiv:1005.1241 [hep-ex]].
 - [32] V. Alvarez *et al.* [NEXT Collaboration], arXiv:1106.3630 [physics.ins-det].
 - [33] J. J. Gomez-Cadenas, J. Martin-Albo, M. Mezzetto, F. Monrabal and M. Sorel, Riv. Nuovo Cim. **35**, 29 (2012) [arXiv:1109.5515 [hep-ex]].
 - [34] A. Giuliani and A. Poves, Adv. High Energy Phys. **2012**, 857016 (2012).
 - [35] O. Cremonesi and M. Pavan, arXiv:1310.4692 [physics.ins-det].
 - [36] V. A. Rodin, A. Faessler, F. Simkovic and P. Vogel, Phys. Rev. C **68**, 044302 (2003) [nucl-th/0305005].
 - [37] V. A. Rodin, A. Faessler, F. Simkovic and P. Vogel, Nucl. Phys. A **766**, 107 (2006) [Erratum-ibid. A **793**, 213 (2007)] [arXiv:0706.4304 [nucl-th]].
 - [38] E. Caurier, F. Nowacki, A. Poves and J. Retamosa, Phys. Rev. Lett. **77**, 1954 (1996).
 - [39] F. Simkovic, A. Faessler, H. Muther, V. Rodin and M. Stauf, Phys. Rev. C **79**, 055501 (2009) [arXiv:0902.0331 [nucl-th]].
 - [40] A. Gando *et al.* [KamLAND Collaboration], arXiv:1303.4667 [hep-ex].
 - [41] S. Kettell, J. Ling, X. Qian, M. Yeh, C. Zhang, C. -J. Lin, K. -B. Luk and R. Johnson *et al.*, arXiv:1307.7419 [hep-ex].
 - [42] S. -H. Seo, Nucl. Phys. Proc. Suppl. **237**, 65 (2013) See also <http://home.kias.re.kr/MKG/h/reno50>.
 - [43] K. Abe *et al.* [T2K Collaboration], Phys. Rev. Lett. **107**, 041801 (2011) [arXiv:1106.2822 [hep-ex]].
 - [44] F. P. An *et al.* [Daya Bay Collaboration], Chin. Phys. C **37**, 011001 (2013) [arXiv:1210.6327 [hep-ex]].

- [45] H. Seo, *Recent Results from RENO*, Talk at XXIV Workshop on Weak Interactions and Neutrinos (WIN 2013), September 16-21, Natal, Brazil.
- [46] J. Wolf [KATRIN Collaboration], Nucl. Instrum. Meth. A **623**, 442 (2010) [arXiv:0810.3281 [physics.ins-det]].
- [47] <http://www-ik.fzk.de/~katrin/publications/documents/DesignReport2004-12Jan2005.pdf>
- [48] P. A. N. Machado, H. Minakata, H. Nunokawa and R. Zukanovich Funchal, arXiv:1307.3248 [hep-ph].
- [49] W. Winter, Phys. Rev. D **70**, 033006 (2004) [hep-ph/0310307].
- [50] P. Huber, M. Lindner and W. Winter, JHEP **0505**, 020 (2005) [hep-ph/0412199].
- [51] G. L. Fogli, E. Lisi, A. Marrone, A. Melchiorri, A. Palazzo, P. Serra and J. Silk, Phys. Rev. D **70**, 113003 (2004) [hep-ph/0408045].
- [52] J. Beringer *et al.* [Particle Data Group Collaboration], Phys. Rev. D **86**, 010001 (2012).
- [53] G. Pantos, F. Simkovic, J. D. Vergados and A. Faessler, Phys. Rev. C **53**, 695 (1996) [nucl-th/9612036].
- [54] J. Kotila and F. Iachello, Phys. Rev. C **85**, 034316 (2012) [arXiv:1209.5722 [nucl-th]].
- [55] H. V. Klapdor-Kleingrothaus, I. V. Krivosheina, A. Dietz and O. Chkvorets, Phys. Lett. B **586**, 198 (2004) [hep-ph/0404088].
- [56] M. Kortelainen and J. Suhonen, Phys. Rev. C **75**, 051303 (2007) [arXiv:0705.0469 [nucl-th]].
- [57] M. Kortelainen and J. Suhonen, Phys. Rev. C **76**, 024315 (2007) [arXiv:0708.0115 [nucl-th]].
- [58] J. Barea and F. Iachello, Phys. Rev. C **79**, 044301 (2009).
- [59] J. Barea, J. Kotila and F. Iachello, Phys. Rev. C **87**, 014315 (2013) [arXiv:1301.4203 [nucl-th]].
- [60] E. Caurier, J. Menendez, F. Nowacki and A. Poves, Phys. Rev. Lett. **100**, 052503 (2008) [arXiv:0709.2137 [nucl-th]].
- [61] J. Menendez, A. Poves, E. Caurier and F. Nowacki, Nucl. Phys. A **818**, 139 (2009) [arXiv:0801.3760 [nucl-th]].
- [62] J. Barea, J. Kotila and F. Iachello, Phys. Rev. Lett. **109**, 042501 (2012).
- [63] M. Wyman, D. H. Rudd, R. A. Vanderveld and W. Hu, Phys. Rev. Lett. **112**, 051302 (2014) [arXiv:1307.7715 [astro-ph.CO]].
- [64] J. Hamann and J. Hasenkamp, JCAP **1310**, 044 (2013) [arXiv:1308.3255 [astro-ph.CO]].
- [65] C. Carbone, L. Verde, Y. Wang and A. Cimatti, JCAP **1103**, 030 (2011) [arXiv:1012.2868 [astro-ph.CO]].
- [66] T. D. Kitching, A. F. Heavens, L. Verde, P. Serra and A. Melchiorri, Phys. Rev. D **77**, 103008 (2008) [arXiv:0801.4565 [astro-ph]].
- [67] L. Amendola *et al.* [Euclid Theory Working Group Collaboration], Living Rev. Rel. **16**, 6 (2013) [arXiv:1206.1225 [astro-ph.CO]].
- [68] J. Hamann, S. Hannestad and Y. Y. Y. Wong, JCAP **1211**, 052 (2012) [arXiv:1209.1043 [astro-ph.CO]].
- [69] C. Kraus, B. Bornschein, L. Bornschein, J. Bonn, B. Flatt, A. Kovalik, B. Ostrick and E. W. Otten *et al.*, Eur. Phys. J. C **40**, 447 (2005) [hep-ex/0412056].
- [70] V. N. Aseev *et al.* [Troitsk Collaboration], Phys. Rev. D **84**, 112003 (2011) [arXiv:1108.5034 [hep-ex]].
- [71] F. Capozzi, G. L. Fogli, E. Lisi, A. Marrone, D. Montanino and A. Palazzo, arXiv:1312.2878 [hep-ph].
- [72] H. Minakata, H. Nunokawa, W. J. C. Teves and R. Zukanovich Funchal, Phys. Rev. D **71**, 013005 (2005) [hep-ph/0407326].
- [73] A. Bandyopadhyay, S. Choubey, S. Goswami and S. T. Petcov, Phys. Rev. D **72**, 033013 (2005) [hep-ph/0410283].
- [74] S. -F. Ge, K. Hagiwara, N. Okamura and Y. Takaesu, JHEP **1305**, 131 (2013) [arXiv:1210.8141 [hep-ph]].
- [75] F. Capozzi, E. Lisi and A. Marrone, Phys. Rev. D **89**, 013001 (2014) [arXiv:1309.1638 [hep-ph]].
- [76] S. R. Elliott and P. Vogel, Ann. Rev. Nucl. Part. Sci. **52**, 115 (2002) [hep-ph/0202264].
- [77] F. T. Avignone, G. S. King and Y. G. Zdesenko, New J. Phys. **7**, 6 (2005).
- [78] F. T. Avignone, III, S. R. Elliott and J. Engel, Rev. Mod. Phys. **80**, 481 (2008) [arXiv:0708.1033 [nucl-ex]].
- [79] M. K. Moe, Nucl. Phys. Proc. Suppl. **19**, 158 (1991).
- [80] O. Host, O. Lahav, F. B. Abdalla and K. Eitel, Phys. Rev. D **76**, 113005 (2007) [arXiv:0709.1317 [hep-ph]].
- [81] S. Hannestad, arXiv:0710.1952 [hep-ph].
- [82] S. Goswami and W. Rodejohann, Phys. Rev. D **73**, 113003 (2006) [hep-ph/0512234].
- [83] S. Goswami and W. Rodejohann, JHEP **0710**, 073 (2007) [arXiv:0706.1462 [hep-ph]].
- [84] I. Girardi, A. Meroni and S. T. Petcov, JHEP **1311**, 146 (2013) [arXiv:1308.5802 [hep-ph]].